Electrocatalysts

International Edition: DOI: 10.1002/anie.201500569
German Edition: DOI: 10.1002/ange.201500569

On the Role of Metals in Nitrogen-Doped Carbon Electrocatalysts for Oxygen Reduction

Justus Masa, Wei Xia, Martin Muhler, and Wolfgang Schuhmann**

Keywords:
carbon · doping · electrocatalysis · metal-free catalysts · oxygen reduction

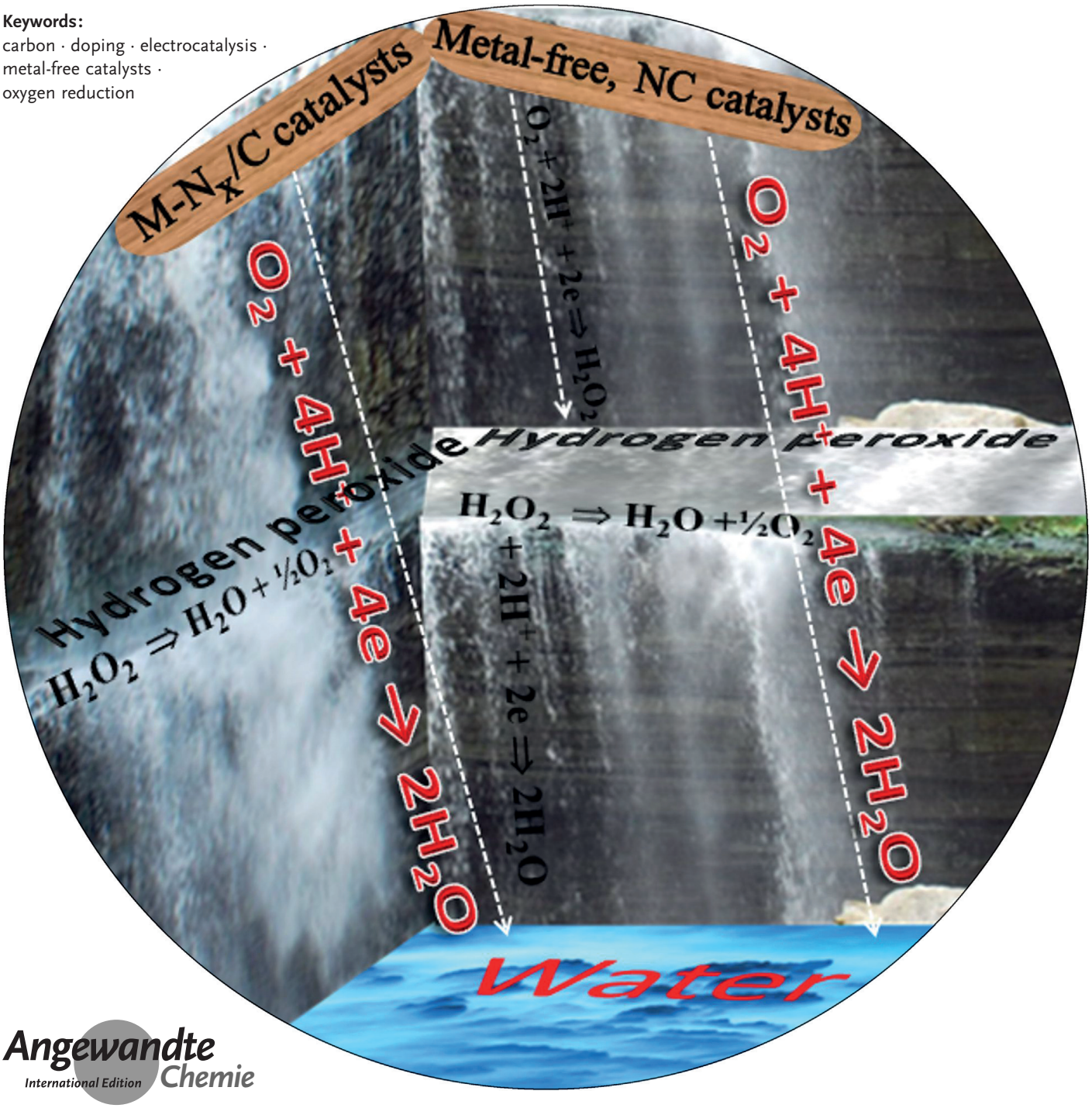

Angewandte International Edition Chemie

The notion of metal-free catalysts is used to refer to carbon materials modified with nonmetallic elements. However, some claimed metal-free catalysts are prepared using metal-containing precursors. It is highly contested that metal residues in nitrogen-doped carbon (NC) catalysts play a crucial role in the oxygen reduction reaction (ORR). In an attempt to reconcile divergent views, a definition for truly metal-free catalysts is proposed and the differences between NC and M-N_x/C catalysts are discussed. Metal impurities at levels usually undetectable by techniques such as XPS, XRD, and EDX significantly promote the ORR. Poisoning tests to mask the metal ions reveal the involvement of metal residues as active sites or as modifiers of the electronic structure of the active sites in NC. The unique merits of both M-N_x/C and NC catalysts are discussed to inspire the development of more advanced nonprecious-metal catalysts for the ORR.

From the Contents

1. Introduction

Carbon materials modified with nonmetallic elements, including boron, fluorine, nitrogen, phosphorus, and sulfur, are of emerging importance in electrocatalysis,[1–9] heterogeneous catalysis,[10] and material science.[11–14] As a consequence of their low cost, these materials are considered as potential replacements for costly catalysts in some vital reactions, for example, as substitutes for platinum for the oxygen reduction reaction (ORR) in fuel cells, metal/air batteries, and in chlor-alkali electrolysis.[1,2,6–9,15–24] Nitrogen-modified carbons (NCs)[9,25–27] have been more intensively investigated as heteroatom-modified carbon catalysts for the ORR than their counterparts modified with boron,[17,28–30] fluorine,[31] phosphorus,[16,23,32,33] and sulfur.[34,35] NC catalysts essentially contain nitrogen incorporated in the carbon structure, either at the edges or within the core structure of the carbon material by replacing one of the sp^2-hybridized carbon atoms in the graphitic structure. Figure 1 shows the various forms of

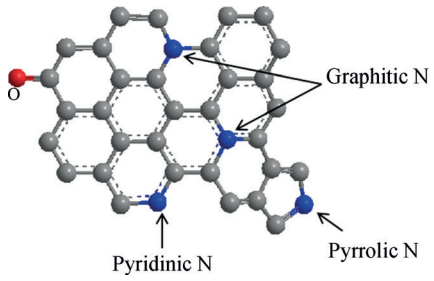

Figure 1. Different forms of nitrogen-functionalized carbon. C gray, N blue, and O red.

NC structures which are considered to be relevant for the ORR. There are contradicting theories about the structure of the active sites of NC catalysts.

Some authors claim that the graphitic species plays the dominant role,[32,36,37] while others contend that the pyridinic species is more active and dominant.[38,39] Some studies propose the involvement of both pyridinic and graphitic species, as well as the pyrrolic species, as active sites.[32,37,40–44]

There is enormous research activity concerned with the development of NC catalysts for the ORR, and the methods used for their synthesis are numerous. The synthesis of NC catalysts can be conveniently grouped into two categories, namely, methods which do not involve the use of any metal precursors and those which make use of metal precursors. Whereas the catalysts produced by the former method may be appropriately classified as metal-free, controversy arises when the catalysts produced by the latter method are designated as "metal-free". This controversy arises because of the close similarity between NC catalysts produced using metal precursors and the M-N_x/C catalysts, where the presence of the metal (M = Co, Fe, or Mn) is considered essential.[45–60] Proponents of the M-N_x/C catalysts believe that the metal ion is involved in the active site, contrary to the theories that claim that the metal ions only facilitate the formation of active sites but do not themselves participate as active sites.[61–64]

It is commonly reported that metal residues in NC catalysts produced using metal precursors are leached out with the aid of mineral acids.[15] However, this is highly contested because of the limitations of the methods employed to determine trace metal impurities at concentrations which are believed to profoundly influence the ORR.[47,48,65–77] In particular, it has been demonstrated that XPS, EDX, and XRD are not sensitive enough to preclude the presence of metal impurities in NC catalysts. Several reports confirm that prolonged treatment of carbon nanotubes (CNTs) prepared

[*] Dr. J. Masa, Prof. Dr. W. Schuhmann
Analytical Chemistry and Center for Electrochemical Sciences (CES)
Ruhr-Universität Bochum
NC04/788, 44780 Bochum (Germany)
E-mail: wolfgang.schuhmann@rub.de
Homepage: http://www.rub.de/elan
Dr. W. Xia, Prof. Dr. M. Muhler
Laboratory of Industrial Chemistry, Ruhr-University Bochum
NBCF 04/690, 44780 Bochum (Germany)
E-mail: Muhler@techem.rub.de

using chemical vapor deposition (CVD) does not rid them of all the metal residues that were used as catalysts.[78,79] In a study by Pumera and Iwai,[75] treatment of multiwalled carbon nanotubes (MWCNTs) with nitric acid at 80 °C only leached out 88 wt % of the metal residues. Relatedly, Kobayashi et al.[64] reported that treatment of a catalyst obtained by pyrolysis of iron phthalocyanine with a phenolic resin polymer at 800 °C in the presence of hydrochloric acid only reduced the Fe content by 36 %. A recent study found that Fe particles encapsulated inside CNTs promote the ORR, and the Fe particles are shielded from dissolution in acid electrolytes by the graphitic layers surrounding them.[67] In separate studies, we were able to unzip and simultaneously oxidize buried metal residues by thermal oxidation after washing nitrogen-doped CNTs (NCNTs) with hydrochloric acid.[80] The resulting partially embedded metal oxides served as excellent catalysts for both the ORR and the oxygen evolution reaction. On the other hand, some presumed metal-free catalysts which are prepared from graphene oxide may contain metal impurities, notably Mn, if Hummer's method is used for the synthesis of the graphene oxide.[75,81,82] The maximum threshold of Fe impurities in CNTs that would be electrochemically insignificant was reported to be in the range of 10 to 100 ppm.[83] Therefore, the designation of NC catalysts produced using metal precursors as "metal-free" should either be avoided or there should be definitive proof of their complete removal or, if present, of their non-involvement in the electrocatalytic reaction of interest.

This Review aims to reconcile divergent views on the role of metal impurities in NC catalysts, and to clarify the validity of the notion of a metal-free catalyst. We therefore 1) propose a definition of a metal-free catalyst, 2) distinguish between M-N_x/C and NC catalysts, 3) highlight research frontiers in the development of NC and M-N_x/C catalysts, and 4) propose perspectives for exploitation of the unique merits of both M-N_x/C and NC catalysts to achieve advanced nonprecious catalysts for the ORR. However, truly metal-free NC catalysts cannot be discussed exhaustively in this Review, which is focused on the impact of often-overlooked trace metal contaminations.

2. Electrocatalysis of Oxygen Reduction

2.1. The Oxygen Reduction Reaction

The electrocatalytic reduction of O_2 in aqueous electrolytes proceeds through one of two generally recognized pathways, as summarized in Equations (i)–(iv).

Acidic medium		Alkaline medium	
$O_2 + 4H^+ + 4e \longrightarrow 2H_2O$		$O_2 + 2H_2O + 4e \longrightarrow 4OH^-$	(i)
$O_2 + 2H^+ + 2e \longrightarrow H_2O_2$		$O_2 + H_2O + 2e \longrightarrow HO_2^- + OH^-$	(ii)
$H_2O_2 + 2H^+ + 2e \longrightarrow 2H_2O$		$HO_2^- + H_2O + 2e \longrightarrow 3OH^-$	(iii)
$H_2O_2 \longrightarrow H_2O + 1/2O_2$		$HO_2^- \longrightarrow OH^- + 1/2O_2$	(iv)

Justus Masa studied Industrial Chemistry at Makerere University in Kampala (Uganda) and completed his BSc in 2003 and MSc in 2008. He finished his PhD in 2012 at Ruhr-University Bochum in the group of W. Schuhmann. He was a Visiting Scholar in the Physical and Theoretical Chemistry Laboratory at the University of Oxford in the summer of 2013. He is currently a postdoctoral researcher at Ruhr-Universität Bochum. His research interests include electrocatalysis, especially the rational design of low-cost catalysts for fuel cells, electrolyzers, and nanomaterials design for electrochemical energy systems.

Wei Xia studied chemistry at Tongji University in Shanghai from 1993 to 1998. After working for four years in Shanghai, he moved to Germany in 2002 and obtained his Master in polymer science from Martin-Luther University Halle–Wittenberg in 2004. He then moved to Ruhr-University Bochum and obtained his PhD in heterogeneous catalysis in 2006 under the supervision of Prof. M. Muhler. Since 2008 he has been a group leader in the Laboratory of Industrial Chemistry, Ruhr-University Bochum.

Martin Muhler studied chemistry at the Ludwig Maximilians University in Munich and received his PhD in 1989 at the Fritz Haber Institute of the Max Planck Society in Berlin with Prof. Dr. G. Ertl. After two years postdoctoral research at the Department of Fundamental Research in Heterogeneous Catalysis at Haldor Topsøe A/S in Denmark, in 1991 he became group head at the FHI Berlin. In 1996, he completed his habilitation in Industrial Chemistry at the TU Berlin, and was appointed full Professor of Industrial Chemistry at the Ruhr University Bochum. In 2013, he was elected Chairman of the German Catalysis Society.

Wolfgang Schuhmann studied chemistry at the University of Karlsruhe, and completed his PhD with F. Korte in 1986 at the Technical University of Munich. After finishing his habilitation at Technical University of Munich in 1993, he was appointed professor for Analytical Chemistry at the Ruhr-Universität Bochum in 1996. He is a fellow of the Royal Society of Chemistry (2005) and the International Society of Electrochemistry (2012). He has received the Biosensors & Bioelectronics Award (2000), the Julius von Haast Fellowship Award (2008), and the Katsumi Niki Prize of Bioelectrochemistry (2012).

In galvanic systems involving O_2 reduction, such as fuel cells, maximum free energy is harnessed when O_2 is reduced by the four electron reduction pathway (i). The reduction of O_2 by the two electron transfer pathway (ii) affords only about half of the energy compared to the four electron reduction pathway. Reaction (i) is favorable on electrocatalytically active surfaces, where rupture of the O–O bond occurs, and involves active sites and geometries which favor dissociative adsorption of O_2, for example, as in the case of the lateral adsorption of oxygen on platinum.[84] At least four modes of interaction of O_2 with a catalytic site have been proposed and they include bridge-cis and bridge-trans interactions, as proposed by Collman et al.[85] and Yeager,[86] respectively, and end-on and side-on interaction, as proposed by Pauling[87] and Griffith,[88] respectively. The bridge-cis and bridge-trans forms of interactions favor rupture of the O–O bond and leads to reduction of O_2 through Equation (i), while end-on and side-on interactions generally favor the formation of H_2O_2 through Equation (ii). The H_2O_2 formed in Equation (ii) may be further reduced to H_2O or OH^- through Equation (iii), or undergo disproportionation according to Equation (iv), thereby regenerating O_2 in the process. Reactions (iii) and (iv) may occur competitively in parallel, depending on the nature of the catalyst, its composition, and properties. Some of the O_2 regenerated in reaction (iv) may be cyclically re-reduced until it is completely reduced to H_2O or OH^-, while a fraction of it may be lost.[48]

The theoretical equilibrium potential for the ORR is 1.229 V (versus RHE) under standard conditions.[89] This reaction is, however, very inefficient in practice and occurs at a considerable overpotential. In addition, the reaction is inherently very slow kinetically because of the coupled multielectron multiproton reactions involving many reaction intermediates and reaction barriers.[90] Overcoming these drawbacks necessitates the use of catalysts. We thus discuss a few of the most important classes of electrocatalysts for the ORR in aqueous electrolytes.

2.2. Types of Catalysts for Oxygen Reduction

2.2.1. Platinum Group Catalysts

The most effective catalysts for the ORR in aqueous electrolytes involve elements of the Pt group, including alloys of Pt and 3d transition metals.[89,91] Platinum itself is by far the most active element for the ORR under both alkaline and acidic conditions. As a consequence of concerns over scarcity and affordability, there has been tremendous research effort to replace Pt with less costly catalysts for the ORR and to improve its utilization through decreased loading.[89,92] Alloying Pt with transition metals has been demonstrated by several groups to cause a significant increase in activity.[84,93] The Pt loading can also be significantly reduced by nanostructuring of the Pt and dispersion on high surface area supports, typically carbon.

However, the grim reality is that even the most ingenious design approaches cannot dispel concerns over the scarcity and cost of Pt. Therefore, the search for non-platinum-based catalysts, also referred to as nonprecious-metal catalysts, has been the effort of many researchers for several decades.[57,58,92,94,95] In the following, we discuss the most promising classes of non-platinum catalysts.

2.2.2. Non-Platinum Catalysts for Oxygen Reduction

One of the earliest classes of non-platinum catalysts for O_2 reduction were complexes with macrocyclic N_4 ligands.[96] A major drawback of these complexes is their low activity as well as low stability in alkaline and acidic electrolytes. They are incapable of sustaining a meaningful current for a reasonable duration under the harsh conditions of fuel cells. Pyrolysis of carbon-supported N_4-macrocyclic complexes at high temperatures, typically between 550 °C and 1000 °C, yields much more active and more stable catalysts, although the macrocyclic structure of the complex is partially or completely destroyed.[97,98] Pyrolyzed N_4-macrocyclic complexes are thus commonly designated as MNC, or M-N_x/C, where M is a 3d transition metal, mostly Fe or Co, and x ($1 \leq x \leq 4$) represents the number of nitrogen atoms coordinated to M.[56,99,100] Interestingly, M-N_x/C-type catalysts can also be prepared by pyrolysis of simple mixtures of metal salts, carbon, and nitrogen precursors.[51,57,58,95,101–103] Metal carbides and nitrides,[43,71] metal oxides,[104,105] and heteroatom-doped carbon materials[7,19,20,106] are other examples of non-platinum oxygen reduction catalysts that have been widely investigated. M-N_x/C catalysts are the most promising class of non-platinum catalysts for the ORR, and also are important in understanding the origin of the controversy of the role of metal entities in NC catalysts.[49]

2.2.3. M-N_x/C Catalysts

It is imperative to give some background on the M-N_x/C catalysts and to describe their relationship with NC catalysts to understand the cause of the controversy of the role of metal entities in NC catalysts on the ORR. M-N_x/C catalysts are the most promising class of non-platinum catalysts for the ORR in acidic and alkaline electrolytes.[57,58,91,92,103,107,108] Traditionally, M-N_x/C catalysts are prepared by pyrolysis of carbon-supported nitrogen-rich metal complexes or mixtures comprising a metal salt, a nitrogen-rich organic compound, and carbon in the presence of ammonia or an inert gas.[98,101,109] Recently, Li et al.[69] reported M-N_x/C catalysts synthesized by controlled oxidation of CNTs to expose buried residual catalysts and subsequent treatment with NH_3 vapor to form M-N_x/C.

The Bao research group[67] reported a Fe-N_x/C-like catalyst with the metal encapsulated inside peapod-like CNTs. Fundamentally, the metal is considered an essential part of the active site in M-N_x/C catalysts.[53–56,110,111] However, nitrogen-functionalized carbon species are also part of the pyrolytic products.

Figure 2 shows a schematic representation of the structural composition of M-N_x/C catalysts prepared by the high-temperature pyrolysis of metal, nitrogen, and carbon precursors. The current theories for the active sites of M-N_x/C-type catalysts are based on the theories first proposed for pyrolyzed N_4-metallomacrocyclic complexes.[54,55,59,99,110,112]

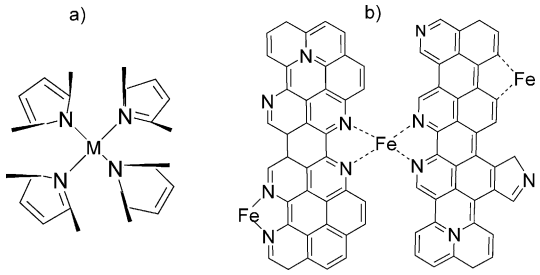

Figure 2. Active sites of a) M-N_4/C and b) Fe-N_2/C and Fe-N_{2+2}/C in M-N_x/C catalysts. Redrawn from Refs. [45] and [115], respectively, with some minor modifications, with permission from the ACS and the AAAS.

According to van Veen et al.,[110] the highest activity of pyrolyzed N_4-metallomacrocyclic complexes supported on carbon is observed at moderate pyrolysis temperatures (500–600 °C). It is believed that the M-N_4 moieties of the complex are conserved and serve as the active sites for the ORR. The Yeager research group[86,113] proposed that decomposition of the N_4-macrocyclic complex commences at about 400–500 °C and is completely dissociated above 800 °C to yield oxides, metallic species, and nitrogen-functionalized species bound on carbon. This group believed that the actual active sites were formed upon contact of the catalyst with an electrolyte, where the metallic and oxide species undergo dissolution and subsequently adsorb or coordinate to nitrogen-containing functional groups on the carbon matrix to form M-N_x-C moieties, which are the active sites. In contrast, Wiesener[114] postulated that the metal ions, Fe or Co, in the N_4-metallomacrocyclic complexes facilitated the decomposition of the nitrogen-rich chelate during pyrolysis at high temperatures, thereby leading to the formation of nitrogen-functionalized forms of carbon, NC, which serve as the active sites. According to this theory, the metal ions were considered to play no role in the ORR.

2.2.3.1. *Oxygen Reduction on M-N_x/C Catalysts*

M-N_x/C catalysts exhibit the most promising activity based on the 2017 milestone for non-platinum based fuel-cell electrocatalysts set by the Department of Energy (DOE). The DOE activity target for 2017 is to achieve an iR-corrected volumetric current density of 300 A cm^{-3} at 0.8 V.[116] Zelenay and co-workers designed M-N_x/C catalysts with outstanding activity by using polyaniline (PANI) as a carbon–nitrogen template and Co and Fe salts.[103] Figure 3 (bottom panel) shows rotating-ring disk electrode (RRDE) data for their catalysts with different compositions and thermal treatment temperatures under N_2. The RRDE data was recorded in H_2SO_4 (0.5 M), with the exception of the Pt/C catalyst which was performed in $HClO_4$ (0.1 M) to avoid suppression of its activity as a result of adsorption of bisulfate anions. Their best catalyst PANI-Fe/C (curve 7) delivered the same current as the state-of-the art catalyst (ETEK-Pt/C) at only 60 mV overpotential. The catalysts pyrolyzed with both polyaniline and the metal salts were considerably more active than those pyrolyzed without any metal Fe or Co precursors.

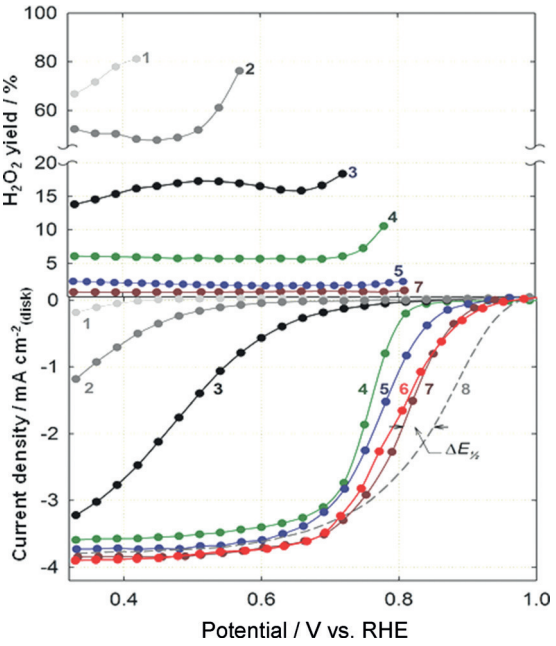

Figure 3. Steady-state ORR polarization curves (bottom) and H_2O_2 yields (top) measured with different polyaniline (PANI) derived catalysts and reference materials: 1. As received carbon black (Ketjenblack EC-300); 2: heat-treated carbon black; 3: heat-treated PANI-C; 4: PANI-Co-C; 5: PANI-FeCo-C(1); 6: PANI-FeCo-C(2); 7: PANI-Fe-C; 8: ETEK Pt/C (20 μg_{Pt} cm^{-2}). Electrolyte: O_2-saturated 0.5 M H_2SO_4 and 0.1 M $HClO_4$ in the case of the experiment with the Pt catalyst. Reproduced from Ref. [103] with permission from the AAAS.

Selectivity measurements reveal that the catalysts pyrolyzed without any metal precursors generate high proportions of H_2O_2. Carbon black without any treatment reduces oxygen nearly exclusively to H_2O_2. Functionalizing the carbon black with nitrogen results in the amount of H_2O_2 being significantly reduced from over 70% to less than 20%. In contrast, all the metal-containing catalysts generated less than 6% H_2O_2. The iron-containing catalysts PANI-FeCo-C (curve 6) and PANI-Fe-C (curve 7) generated less than 1% H_2O_2. The catalysts with both Fe and Co (PANI-FeCo-C) showed excellent performance in a H_2/O_2 fuel cell (Figure 4), approaching the performance of Pt/C. In addition, a stable performance was sustained for at least 700 h at 0.4 V. TEM studies revealed that the catalyst was comprised of metal particles encapsulated inside onionlike graphitic carbon nanoshells.

A review by Jaouen et al.[57] compared the physicochemical properties of M-N_x/C catalysts prepared in different leading laboratories and found that their mass activity was in the range of 10–20 A g^{-1} at 0.8 V versus the reversible hydrogen electrode (RHE). Only one catalyst reached a mass activity of 80 A g^{-1}, or 19 A cm^{-3}, which corresponds to one-seventh of the 2010 DOE target of 130 A cm^{-3}.[117] This study concluded that the activity of the catalysts was limited by the area of the microporous surface and not the absolute amount of metal (Fe or Co) and nitrogen in the catalysts. A low density of active sites is attributed to be one of the causes of the relatively lower performance of M-N_x/C catalysts

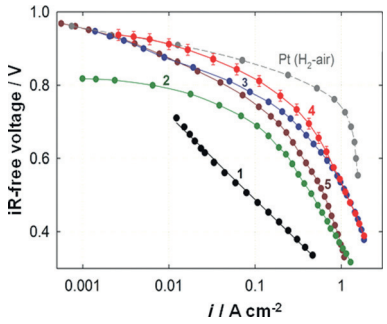

Figure 4. Polarization curves for the H_2/O_2 fuel cell recorded with various PANI-derived cathode catalysts at a loading of 4 mg cm^{-2}. 1: PANI-C; 2: PANI-Co-C; 3: PANI-FeCo-C(1); 4: PANI-FeCo-C(2) (standard deviations from three independent measurements marked for all data points); 5: PANI-Fe-C. The performance of the H_2/air fuel cell with a Pt cathode (0.2 mg Pt cm^{-2}) is shown for comparison (dashed line). All tests used a Pt/C catalyst at a loading of 0.25 mg Pt cm^{-2} at the anode; anode and cathode gas pressure: 2.8 bar. Reproduced from Ref. [103] with permission from the AAAS.

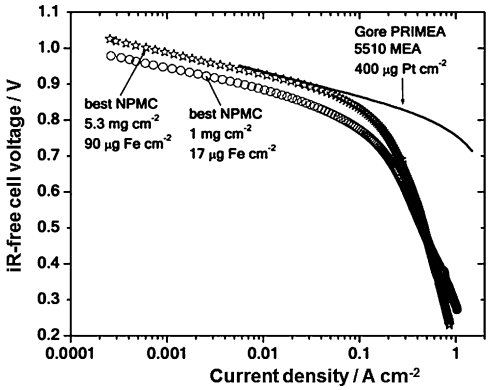

Figure 5. Polarization curves of a H_2/O_2 fuel cell with the cathode based on a Fe-N_x/C catalyst at a loading of 1 mg cm^{-2} (circles) and 5.3 mg cm^{-2} (stars). Also included is a ready-to-use Gore PRIMEA membrane electrode assembly (MEA; W. L. Gore & Associates) with ca. 0.4 mg Pt cm^{-2} at the cathode and anode. Reproduced from Ref. [107] with permission from the AAAS.

compared to platinum, especially at low overpotentials, as can be seen in Figure 3.

A remarkable effort to overcome this drawback was reported by Lefèvre et al.,[107] who employed planetary ball-milling to fill the micropores of carbon black with 1,10-phenanthroline or perylenetetracarboxylic dianhydride (PTCDA) and iron acetate followed by pyrolysis, first in argon then in ammonia. The best catalyst synthesized by this method achieved a volumetric current density of 99 A cm^{-3}, which at the time was very close to the 2010 DOE target of 130 A cm^{-3}.[117] The main results of this study are summarized in the H_2/O_2 fuel cell test data presented in Figure 5. It is worth noting that the catalyst attained the same performance as platinum at a cathode loading of 5.3 mg cm^{-2}. The Fe content in this catalyst was 1.7 %, which corresponds to a Fe loading of 17 µg cm^{-2} for a 1 mg cm^{-2} catalyst loading. However, the catalyst suffered severe diffusion limitation at higher current densities as a result of mass transport limitations within the relatively thick catalyst layer. Durability studies showed that only 59 % of the initial fuel cell (H_2/O_2) performance was retained after 100 h when operating at 0.5 V.

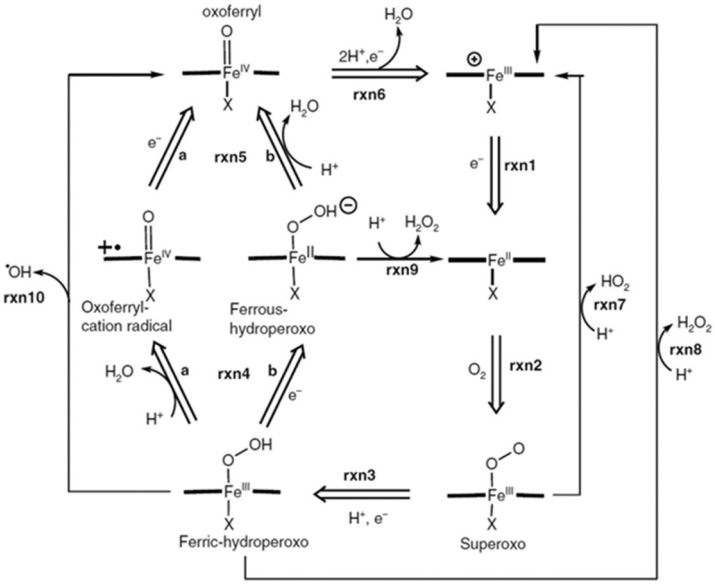

Figure 6. Proposed mechanism for the electrochemical reduction of oxygen catalyzed by Fe porphyrins. Reproduced from Ref. [82] with permission from Springer Science + Business Media

More recently, a catalyst derived from a composite of iron acetate, phenanthroline, and a zeolitic-imidazolate framework was reported with a power density of 0.75 W cm^{-2} and volumetric current density of 230 A cm^{-3}, very close to the DOE 2017 target of 300 A cm^{-3}.[118] In this case, the zeolitic-imidazolate framework served as the microporous host for phenanthroline and iron acetate to achieve a high density of active sites and increase mass transport during O_2 reduction.

2.2.3.2. *Mechanism of O_2 Reduction on M-N_x/C Catalysts*

Most theoretical and experimental studies support the prevalence of a redox-type mechanism for oxygen reduction on M-N_x/C catalysts, similar to the mechanism proposed for O_2 reduction on Fe porphyrins (Figure 6).[119,120]

According to this mechanism, the initial step of O_2 reduction involves its adsorption on the active site, which is considered to be Fe in the ferrous state (Fe^{2+}). In aqueous electrolytes the Fe^{2+} ion is hydrated and exists in the form of Fe^{II}-OH_2, with four nitrogen atoms of the form represented in Figure 2 and an axial ligand X being additionally coordinated to the metal. If Fe is initially in the ferric state (Fe^{3+}), a reduction step $Fe^{3+} \rightarrow Fe^{2+}$ (reaction 1) must precede the O_2 adsorption step. According to Anderson and Sidik,[120] H_2O bonds strongly to the Fe^{3+} site, thus blocking it against O_2 adsorption, but it does not bond strongly to Fe^{2+}, thus making it possible for the O_2 to displace H_2O from Fe^{II}-OH_2 to form

a ferric hydroperoxo adduct (reactions 2 and 3). The intermediate formed according to reaction 4 may react further either through reaction 8 to form H_2O_2 or through reaction 4 depending on the adsorption energy of *OOH. Weakly bound *OOH will desorb from the surface of the catalytic site by reacting with a proton to form H_2O_2 (reaction 8). For relatively strongly bound *OOH, the intermediate may react with a proton to form H_2O and an oxoferryl cation radical (reaction 4a), which reacts further to form an oxoferryl species (reaction 5b), then a ferric species (reaction 6) to regenerate the original Fe^{III} species. Alternatively, the ferric-hydroperoxo intermediate may proceed through reaction 4b to form H_2O_2 and ferrous-hydroperoxo then back to the Fe^{II}-OH_2 through reaction 9 to repeat the cycle.

The interconversion of Fe^{2+} and Fe^{3+} during oxygen reduction has been observed experimentally by in situ X-ray absorption spectroscopy coupled to electrochemical measurements (Figure 7a), thus justifying the validity of the redox mechanism for the ORR on M-N_x/C-type catalysts, especially for the case of Fe-containing catalysts.[121]

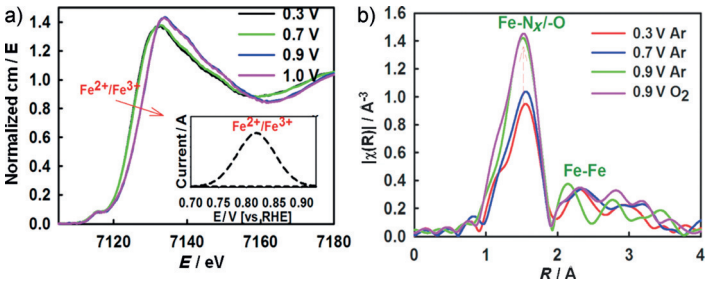

Figure 7. a) Potential-dependent normalized Fe K-edge XANES spectra with corresponding redox peak transition shown in the inset as a background-subtracted square-wave voltammetry profile collected in oxygen-free 0.1 M $HClO_4$. b) Fourier Transform of the extended region of the XAS spectra collected in situ at the Fe K-edge (7112 eV) of a PVAG-Fe catalyst. Reproduced from Ref. [121] with permission from the ACS.

The Fe K-edge XANES spectra shows redox transition of Fe from Fe^{3+} at high potentials to Fe^{2+} at lower potentials in the potential window of 0.7 V to 0.9 V versus RHE, in agreement with the results of square-wave voltammetry shown in the inset of Figure 7a. The redox transition from Fe^{2+} to Fe^{3+} is accompanied by the formation of oxygenated adsorbates (O-Fe^{3+}-N_x) as deduced from the increase in the intensity of the FT XAS peak at about 1.5 Å at potentials above 0.7 V (Figure 7b), with a maximum intensity at 0.9 V. The authors concluded that these observations provided unequivocal evidence of the direct involvement of a redox transition of the metal ion in initiating the reduction of oxygen.

3. Metal-Free Catalysts

3.1. Definition

A metal-free catalyst in the strictest sense is a catalyst which is not composed of any metal elements or, if it should contain such elements, their presence should not influence the properties of the catalyst. Additionally, if the preparation of a metal-free catalyst involves the use of metal precursors, there should be definitive proof that no metal residues are present in the catalyst or, if present, that their presence does not influence its electrocatalytic properties.

The most common metal-free catalysts for oxygen reduction are comprised of carbon modified with at least one nonmetal element, for example, nitrogen, boron, fluorine, phosphorus, or sulfur. Simultaneous modification of carbon with at least two such elements, for example, boron and nitrogen, is reported to further enhance the ORR activity compared to functionalization with only one of the individual elements.[4,13,16,17,28,34,122,123] In the case of nitrogen-modified carbon (NC) catalysts, electrocatalytic enhancement has been suggested to be due to a dipole effect, whereby the electron density of the carbon atoms adjacent to the nitrogen atom is lowered, thus favoring dissociative chemisorption of oxygen.[15,124] As for boron-doped carbon catalysts, activity enhancement is assumed to be the result of electron enrichment of the carbon atoms adjacent to boron as a result of the higher electronegativity of carbon relative to boron.[30] The formed B^+ is believed to favor dissociative adsorption of oxygen, thereby leading to four-electron reduction of O_2. Yang et al.[30] thus proposed that the presence of heteroatoms in carbon causes charge redistribution, regardless of the electronegativity of the doping element. Catalytic enhancement as a result of multiple element doping was proposed by Zheng et al.[17] to be due to a synergistic effect and a higher density of active sites. On the other hand, Cheon et al.[125] reported that the improvement in activity of heteroatom-doped carbon catalysts was related to variation of the work function of carbon as a consequence of the dopant atoms. Metal-free NC catalysts have also been prepared from carbon materials modified with polyelectrolytes, such as poly(diallydimethylammonium chloride) (PDDA).[126] In these catalysts, oxygen reduction is reported to be promoted by intramolecular charge transfer from the carbon matrix to the PDDA.[126] Zhang and Xia[124] proposed on the basis of their density functional theory calculations on nitrogen-doped graphene that any chemical species in the form of a substitution or attachment on graphene which induces high asymmetric spin density and atomic charge density could promote high electrocatalytic activity for the ORR.

3.2. Nitrogen-Doped Carbon (NC) Catalysts

The method used for the synthesis of NC catalysts depends on the properties and type of carbon used as well as the desired properties of the final catalyst.[7–9,12,19–21,127] The carbon materials include carbon blacks, multi-walled carbon nanotubes (MWCNTs), single-walled carbon nanotubes (SWCNTs), mesoporous carbon, and graphene. The methods for the synthesis of NC catalysts can generally be grouped in two categories, namely, direct growth and postsynthesis. In direct growth, the doping of carbon with nitrogen takes place

during the synthesis of the carbon nanostructures. A typical example of this method is chemical vapor deposition (CVD) of a volatile nitrogen-containing organic compound, using metals, typically iron or cobalt, as catalysts.[12,14,128–130]

In situ CVD methods generally produce nitrogen-doped nanotubes or nanofibers or nitrogen-doped graphene.[128] The postsynthetic approach involves treatment of carbon (graphene, CNTs, carbon black) with a reactive nitrogen agent, for example, with a nitrogen plasma or ammonia gas.[36,41] Müllen and co-workers[131] reported the synthesis of hierarchically porous nitrogen-doped carbon using nitrogen-rich aromatic polymers as nitrogen and carbon sources and colloidal silica as a template. In a related study, the same group also reported the synthesis of 3D-hierrachical porous NC catalysts with a super-high surface area (2191 $cm^2 g^{-1}$) by using polydopamine-modified mixed cellulose ester filter films as a sole template, in what they termed "mussel-inspired surface chemistry".[106]

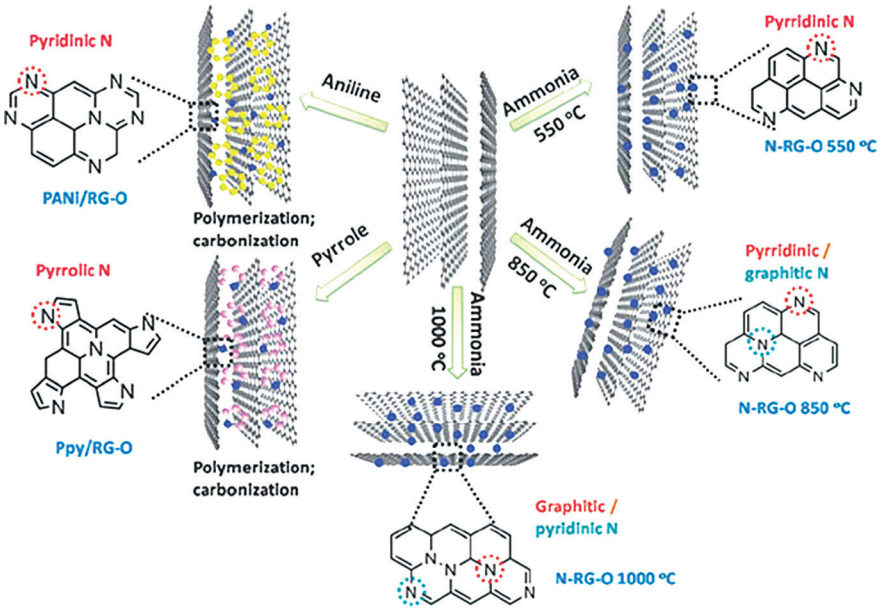

Figure 8. Preparation of nitrogen-doped graphene to give different forms of nitrogen-functionalized carbon. N-RGO 550, 850, and 1000 °C were prepared by annealing graphene oxide (G-O) at 550 °C, 850 °C, and 1000 °C under NH_3. PANi/RG-O and Ppy/RG-O were prepared by annealing composites of polyaniline and polypyrrole, respectively, with G-O at 850 °C. Reprinted from Ref. [32] with permission from the RSC.

Mesoporous NC catalysts with very high surface areas (BET > 1500 $m^2 g^{-1}$) prepared by carbonization of nitrogen-rich compounds and biomass materials including carbohydrates and nucleobases dissolved in ionic liquids have been reported by Antonietti and co-workers.[132–134] NC catalysts are nowadays widely prepared by controlled degradation of nitrogen-rich biomass at high temperatures under an inert gas or by reaction with a reactive nitrogen carrier such as ammonia.[135,136]

To understand the intrinsic activity of the different forms of nitrogen-functionalized carbon, it would be desirable to achieve the tailored synthesis of specific forms of the nitrogen-modified carbon.[27] This, however, turns out to be a very challenging task. Many syntheses invariably yield 2–3 types of nitrogen functionalization, so that the product contains a mixture of graphitic, pyridinic, and pyrrolic species.

There are a few examples which demonstrate the controlled selective synthesis of specific functional groups.[44,137] For example, Figure 8 summarizes an example of the tailored synthesis of pyrrolic, pyridinic, and graphitic carbon reported by Lai et al.[32] In particular, it was observed that annealing graphene oxide with ammonia preferentially formed graphitic and pyridinic nitrogen centers, while annealing a composite of polyaniline with reduced graphene oxide and polypyrrole with reduced graphene oxide tended to generate pyridinic and pyrrolic nitrogen moieties, respectively.

There is wide disagreement in the literature, from both experimental and theoretical perspectives, on the nature of the active sites of NC catalysts, and the relative importance of the pyridinic, graphitic, and pyrrolic nitrogen groups, including the the role of defect sites.[138] For example, a combined experimental and theoretical study by Sidik et al.[36] on the electrocatalysis of oxygen reduction on nitrided Ketjenblack concluded that the active sites for oxygen reduction in H_2SO_4 (0.5 M) were carbon radical sites formed adjacent to nitrogen in the graphite structure, and H_2O_2 peroxide was the main product of oxygen reduction. The authors also concluded that substitutional nitrogen atoms far from the graphite sheet edges were active, while those close to the edges were less active. Meanwhile, DFT calculations performed by Okamoto[43] concluded that the adsorption energy on N-doped graphene becomes energetically favorable as the number of N atoms around a C=C bond increases and that both the $4e^-$ and the $2e^-$ electron transfer pathways are feasible.

On the basis of this model, one may conclude that carbon nitride should posses very high ORR activity and be able to selectively reduce O_2 to water through the four electron transfer pathway. However, experimental studies by Lyth et al.[139] are not consistent with the prediction by Okamoto. Kim et al.[37] proposed a mechanism where both pyridinic and graphitic nitrogen atoms are involved in one catalytic cycle during oxygen reduction (Figure 9). According to this mechanism, the outermost graphitic nitrogen atom provides the most favorable energetics and electron-transfer conditions to facilitate the reduction of O_2 selectively through the four electron transfer pathway rather than the two electron transfer pathway. In the course of the reaction, the graphitic nitrogen atom is believed to convert into pyridinic-like nitrogen atoms in a subsequent coupled electron-proton transfer step through breaking of a C–N bond.

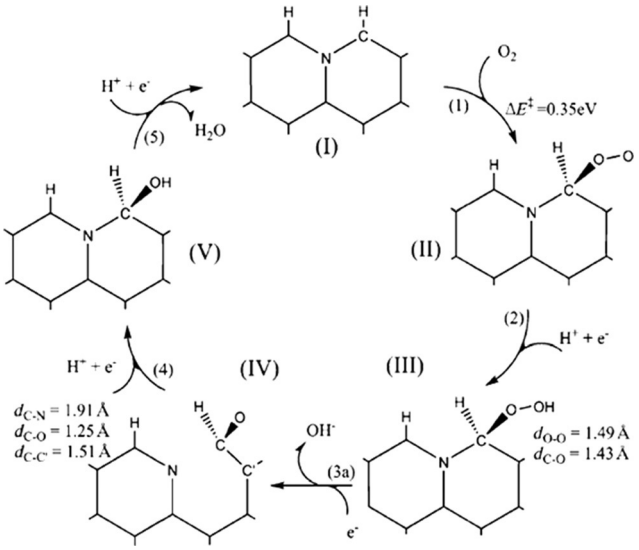

Figure 9. The proposed ORR catalytic cycle with nitrogen at a graphitic edge site. The catalytic cycle shows only the catalytically active part of a graphene nanoribbon (GNR) edge. Arabic numerals next to the arrows in parentheses denote the reaction steps. Reproduced from Ref. [37] with permission from the RSC.

3.3. Origin of the Controversy of the Role of Metals

One of the most influential publications on metal-free catalysts for oxygen reduction was by Gong et al.[15] In this study, vertically aligned nitrogen-containing CNTs (VA-NCNTs) were synthesized by pyrolysis of iron(II) phthalocyanine. The residual metal catalyst was removed by acid leaching.

The authors concluded on the basis of the absence of a signal from Fe during XPS analysis that the residual metal catalyst was completely removed by the acid-washing procedure. The resulting catalyst exhibited higher activity for the ORR in KOH (0.1M) than Pt/C, the state-of-the-art catalyst for oxygen reduction (Figure 10). The authors proposed that the incorporation of electron-accepting nitrogen atoms in the conjugated nanotube carbon plane apparently imparts a relatively high positive charge density on the adjacent carbon atoms, which acts as the active sites.

Winther-Jensen et al.[140] reported fast oxygen reduction on a vapor phase polymerized PEDOT electrode synthesized using iron(III) *para*-toluenesulfonate ($Fe^{III}PTS$) as the oxidant. The involvement of Fe in the electrocatalytic reduction of O_2 was precluded on the basis of CO poisoning tests. This study, however, contradicts observations that the presence of CO does not poison Fe active sites.[141–143]

Metal-free NC catalysts have mostly been investigated in alkaline electrolytes, where they show more promising performance.[1,2,5,7,9,19,20,22,24,25,106,133,136,144,145] Studies in electrolytes with a low pH value show drastically lower activity.[146–148] M-N_x/C catalysts were developed in the late 1970s and became widely investigated in the 1980s. Throughout the 1980s, it was widely believed that both the metal and nitrogen were crucial for the formation of active sites.[55,101,110] However, a group led by Wiesener[114] dispelled the involvement of the metal in the active sites. Bouwkamp-Wijnoltz et al.[45] noted that high-temperature pyrolysis of M, N, and C precursors produces considerable site heterogeneity in electronic terms and that only a fraction of the Fe-N_4 sites were involved in the electrocatalytic reduction of O_2. Kobayashi et al.[62] pyrolyzed a mixture of cobalt phthalocyanine and a phenol resin polymer at 1000 °C and they employed X-ray absorption fine structure (XAFS) analysis and hard X-ray photoemission spectroscopy (HXPES) to probe the composition of the resulting catalysts before and after acid washing. The authors observed that the catalyst contained metallic cobalt after pyrolysis, which was not completely removed by acid washing. However, despite clearly observing residual cobalt, the authors ruled out its involvement as part of the active sites nor its indirect contribution in the electrocatalytic process. In a related study involving the pyrolysis of a mixture of iron phthalocyanine and a phenol resin polymer at 800 °C, the same authors observed that acid washing removed only 36 % of the available Fe.[64] The residual Fe existed in the form of carbide (Fe_3C), which the authors claimed to accelerate the growth of sp^2-hybridized carbon during pyrolysis. Acid washing did not alter the electrochemical properties of the catalysts, which led the authors to conclude that the metal residues did not participate in the oxygen reduction.

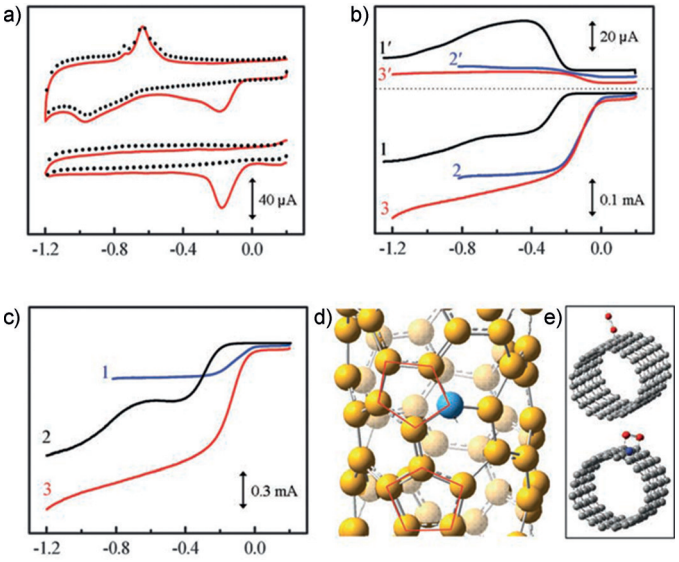

Figure 10. a) Cyclic voltammograms for oxygen reduction at the unpurified (upper) and electrochemically purified (bottom) VA-NCNT/GC electrodes in argon-protected (dotted curves) or air-saturated 0.1 M KOH (solid red curves) at a scan rate of 100 $mV s^{-1}$. b) RRDE voltammograms and the corresponding amperometric responses for oxygen reduction in air-saturated 0.1 M KOH at the NA-CCNT/GC (curves 1 and 1′), Pt-C/GC (curves 2 and 2′), and NA-NCNT/GC (curves 3 and 3′) electrodes at a scan rate of 10 $mV s^{-1}$, 1400 rpm, with a ring potential of 0.5 V. c) RRDE voltammograms for oxygen reduction in air-saturated 0.1 M KOH at Pt-C/GC (curve 1), VA-CCNT (curve), and VA-NCNT (curve 3) electrodes. d) Calculated charge density distribution for the NCNTs. e) Possible adsorption modes of an oxygen molecule at the CCNTs (top) and NCNTs (bottom). Reproduced from Ref. [15] with permission from the AAAS.

3.4. Effect of Acid Washing

Carbon materials are often treated with mineral acids to remove metal residues.[15,42,149,150] However, Pumera[79] noted that the treatment of MWCNTs and SWCNTs with concentrated HNO_3 at 80 °C removed a maximum of 88 wt % of the residual metal impurities. It was concluded on the basis of this finding that treatment of CNTs with HNO_3 removes most of the surface metal impurities, but not metal impurities encased within the CNTs. Jurkschat et al.[78] observed that even prolonged acid washing (for at least 36 h in 2 M HNO_3), which they termed "super washing", did not lead to complete removal of iron impurities from SWCNTs. In a related finding, in which an NC catalyst synthesized by CVD of acetonitrile using Fe as the growth catalyst was washed in 1 M HCl for up to one week, the residual Fe (determined using ICP-OES) initially decreased but then reached a steady state, where further washing did not leach out any more Fe. This led to the conclusion that the Fe which could not be removed was encased inside the carbon and thus not accessible to the acid.[66] Partial oxidation of the CNTs to expose buried metal species followed by acid leaching was proposed to increase the efficiency of the removal of metal residues. However, this was observed to destroy the CNTs.[149] Harutyunyan et al.[151] proposed an approach for the purification of SWCNTs which involved microwave treatment followed by refluxing in 4 M HCl. This procedure significantly reduced the amount of metal residues to 0.2 wt % (ca. 0.04 atom %). It is important to note that even such an aggressive treatment, which is detrimental to the integrity of the SWCNTs, could not completely remove all the metal residues. Therefore, acidic treatment alone does not thoroughly remove all the metal impurities from carbon materials, especially when the metals are encapsulated inside CNTs or protected by graphitic layers.

3.5. Methods for Accurate Determination of Trace Metals

The accuracy of the determination of trace metals is very much dependent upon the method employed. Probably, for reasons of ease of accessibility, X-ray photoelectron spectroscopy (XPS), X-ray diffractometry (XRD), thermogravimetry, inductively coupled plasma-optical emission spectroscopy (ICP-OES), and scanning/transmission electron microscopy (S/TEM) with energy dispersive X-ray analysis are the mostly commonly used techniques for probing metal residues in NC catalysts. However, these might not suffice to determine residual metals at very low concentrations, especially when the metals are encapsulated inside graphitic layers, as in the case of CNTs. Metal particles inside CNTs may remain electrochemically addressable. For example, a recent study by Bao and co-workers[67] found that Fe particles inside CNTs promote the electrocatalytic reduction of O_2. We demonstrated that XPS was incapable of detecting the presence of 0.1 wt % Fe in nitrogen-functionalized carbon black, a concentration which considerably promoted the reduction of O_2.[47,48] Kolodiazhnyi and Pumera[77] gave a critical analysis of the accuracy of a variety of methods for the determination of metal impurities in CNTs. The authors recommend ICP-OES as one of the most reliable methods for the determination of metal impurities in carbon materials. However, the accuracy of ICP-OES depends very much on the sample pretreatment process.[152] Microwave-assisted digestion was recommended to increase the reliability of ICP-OES.[152] However, it should be noted that microwave-assisted digestion demands the use of larger volumes of the acid and longer digestion times. Nevertheless, this may be overlooked if accuracy is the ultimate objective. Besides ICP-OES, other methods that are capable of detecting ppm amounts of metal residues with reasonable accuracy include neutron activation analysis (NAA), magnetic susceptibility, and X-ray fluorescence analysis (XRF).[77]

4. Comparison of Metal-Free and Metal-Containing NC Catalysts

Throughout the 1980s and 1990s, and before 2010, most of the research on the ORR focused on acidic electrolytes because of the great interest in the development of proton exchange membrane (PEM) fuel cells during this period.[84,112] The great interest in PEM fuel cells was propelled by the discovery and popularity of Nafion, a sulfonated tetrafluoroethylene-based polymer which is chemically and mechanically very stable and has a high proton conductivity.[153] The deployment of Nafion as an acidic solid electrolyte yielded fuel cells with a high energy density and which did not suffer from many of the problems that hampered the widespread use of alkaline fuel cells, despite their early success in space exploration missions. However, there has been a resurgence of interest in the electrocatalytic reduction of O_2 in alkaline electrolytes for about a decade. This interest is driven by the improved design of modern alkaline fuel cells and the prospect of developing competitive hydroxide-exchange membranes.[154,155] Electrocatalytic reduction of O_2 under alkaline conditions benefits from the fact that, because the reaction is faster under alkaline conditions, several classes of nonprecious-metal catalysts can satisfactorily substitute platinum.[154] At the height of interest in nonprecious catalysts for PEM fuel cells, M-N_x/C catalysts were the most promising, and a wealth of literature data exists on the electrocatalytic properties of oxygen using M-N_x/C catalysts in acidic electrolytes compared to similar studies in alkaline electrolytes.[89] Despite metal-free catalysts having only recently been discovered, progress on their development has been remarkable and there is widespread intensive research activity in this field.[1–7] These developments benefit from improved understanding of the crucial structural properties that influence activity.[32] It has to be stressed that most studies of oxygen reduction on metal-free catalysts have been performed in alkaline electrolytes, where the catalysts apparently show promising competitiveness in relation to M-N_x/C and Pt-based catalysts. Therefore, in discussing the role of metals in NC, we present examples for acidic and alkaline electrolytes separately.

4.1. ORR on NC and M-N_x/C Catalysts in Acidic Electrolytes

In acidic electrolytes, totally metal-free NC catalysts perform considerably worse than M-N_x/C and Pt-based catalysts, with H_2O_2 being the main product.[134,156,157] Figure 11 shows a compilation from at least 30 literature sources, expounding on the data reported by Dodelet[49] and others[158–161] of the average potential corresponding to a current density of -1 mA cm^{-2} for metal-free NC, M-N_x/C (M = Co and Fe), and Pt-based catalysts.

Irrespective of the type of electrolyte, the results clearly indicate that the catalysts containing either Co or Fe are much more active than metal-free NC catalysts. The average potential of metal-free catalysts in acidic electrolytes (0.52 V) is lower than that of Fe-N_x/C catalysts (0.83 V) by at least 0.31 V and that of Pt-based catalysts (0.93 V) by at least 0.41 V. These differences become smaller in alkaline electrolytes, although the superiority of the M-N_x/C and Pt-based catalysts is maintained. Although it is apparent from this summary that the presence of either Co or Fe decreases the overpotential for O_2 reduction, it does not directly answer the question of whether the metals are essential entities of the active sites or not, and, if they indeed are, whether they are intrinsically more active than the active sites of metal-free NC catalysts.

4.2. ORR on NC and M-N_x/C Catalysts in Alkaline Eectrolytes

Examples of the role of metals on the electrochemical ORR activity of nitrogen-doped carbon catalysts in alkaline electrolyte are illustrated in Figure 12. It is noteworthy that differences in experimental standards across laboratories give rise to widespread discrepancy in literature data.

A notable challenge is inconsistency in the presentation and interpretation of rotating disc electrode (RDE) and rotating-ring disc electrode (RRDE) measurements designed for kinetic analysis of the ORR. The nitrogen-doped graphene (NG) in Figure 12a was prepared by pyrolysis of exfoliated graphene (Ex-G) with urea, while iron(II) acetate was added to the pyrolysis mixture for the composite Fe-NG. On the basis of Levich's Equation for RDE voltammetry, $i_D = 0.62nFAD^{2/3}\upsilon^{-1/6}C\omega^{1/2}$, where i_D is the diffusion limited current, n is the number of electrons transferred, F is Faraday's constant (96485 C mol^{-1}), D is the diffusion coefficient of oxygen in KOH (0.1 M), ν is the kinematic viscosity of the electrolyte, C is the concentration of oxygen in the electrolyte, and ω is the angular velocity of electrode rotation,

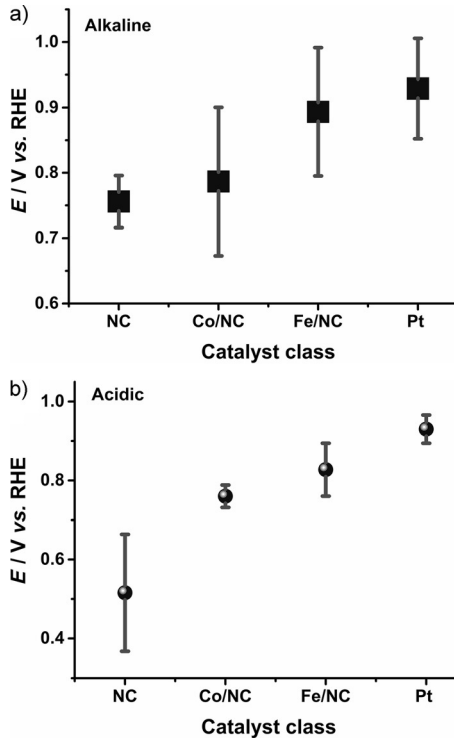

Figure 11. A plot of the average potential (RHE) corresponding to a current density of -1 mA cm^{-2} compiled from at least 30 literature sources, including the data reported by Dodelet[49] and others.[159–161]

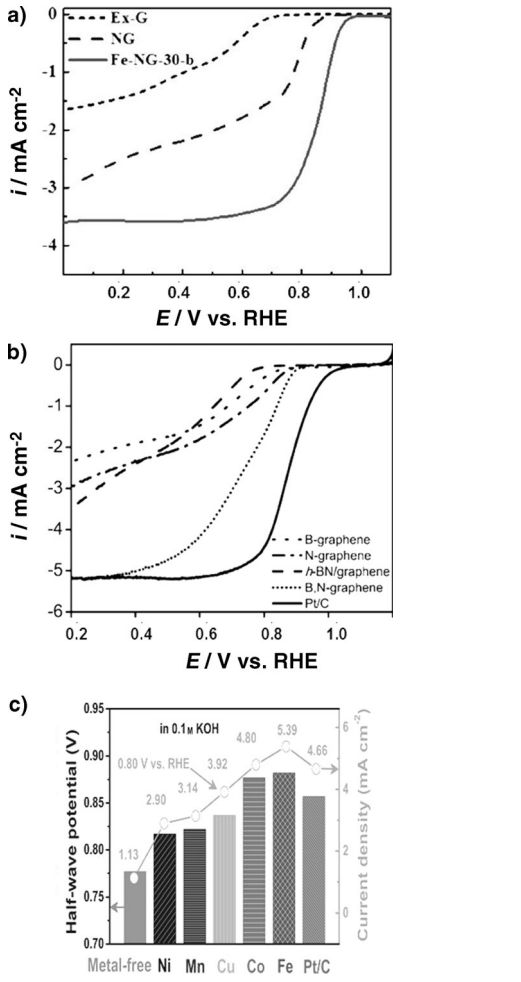

Figure 12. a) Voltammograms recorded at 10 mV s^{-1} and 900 rpm in oxygen-saturated KOH (0.1 M) of thermally exfoliated graphene (Ex-G), nitrogen-doped graphene (NG), and a composite of NG containing Fe. Reproduced from Ref. [161] with permission from the ACS. b) Voltammograms at 10 mV s^{-1} and 1500 rpm in O_2-saturated KOH (0.1 M) boron-doped graphene (B-graphene), nitrogen-doped graphene (N-graphene), hexagonal boron nitride (*h*-BN-graphene), graphene co-doped with boron and nitrogen (B,N-graphene, and Pt/C. Reproduced from Ref. [17] with permission from Wiley. c) Comparison of the ORR activities of NC containing various metals. Reproduced from Ref. [162] with permission from the ACS.

and assuming $C = 1.2 \times 10^{-6}$ mol cm^{-3}, $D = 1.9 \times 10^{-5}$ cm^2 s^{-1}, and $\nu = 0.011$ cm^2 s^{-1}, the diffusion-limited current would be expected to be around 2.85 and 5.7 mA cm^{-2}, respectively, for two- and four-electron reduction of O_2 at a rotation speed of 1600 rpm.[48] By using these values as a quick estimation, one sees that NG would reduce O_2 predominantly through the two electron transfer process, while the reduction of O_2 on Fe-NG would follow an intermediate mechanism between two and four electrons.

To a large extent, most NC catalysts prepared without the involvement of any metal precursors reduce oxygen through the two electron transfer step, thereby leading to the formation of hydrogen peroxide, or through a mechanism involving both the four and the two electron transfer steps, with the average number of electrons being between two and four.[25,123] One notable feature of nitrogen-doped carbon catalysts which is rarely discussed is their high activity towards the decomposition of hydrogen peroxide.[48,52,129]

Maldonado and Stevenson[129] performed analysis of the heterogeneous decomposition of hydrogen peroxide at N-doped carbon nanofibers (N-CNFs) and observed that the rate of decomposition of hydrogen peroxide on N-CNFs was tremendously increased by about 100 fold relative to the nondoped CNFs. We observed in a recent study that metal-free NC catalysts disproportionate hydrogen peroxide nearly as fast as Fe-N_x/C catalysts and that decomposition of hydrogen peroxide is an important reaction step in the reduction of O_2 on this type of catalysts.[48]

The results reported in Figure 12b also support the electroreduction of O_2 by the two electron transfer pathway on N-graphene, as estimated from the diffusion-limited current on the basis of Levich's RDE Equation, and there are a number of reports consistent with these examples.[9,16,38,44,47,48,65,109,126,136,163,164] In Figure 12c, the catalytic activity of a metal-free NC catalyst is seen to be extremely enhanced in the presence of transition metals.[162] Catalytic enhancement has also been observed to increase with metal loading up to a certain point.[46,48,72,159] The ORR activity of metal-free catalysts is generally considerably lower than that of Pt/C (Figure 12b) and there are many similar examples in the literature.[63,65]

The essential parameters necessary for a high ORR activity of NC catalysts include a high active site density, high surface area, a high porosity to facilitate mass transport, and a high degree of graphitization to achieve high electrical conductivity.[21,25,106] Therefore, discrepancy between the results on the selectivity of the ORR on NC catalysts could be partly explained on the basis of differences in these factors. The properties of the carbon matrix used are, therefore, very crucial. To achieve a high active site density, the amenability of a given carbon matrix to functionalization is, therefore, perhaps even more crucial than the nature of the carbon matrix itself. As a consequence of the hydrophobic nature of carbon, its oxidation to introduce oxygen groups on the surface renders it more hydrophilic and hence more amenable to further functionalization.[165] Oxidative pretreatment of carbon has actually been demonstrated to yield catalysts with enhanced ORR activity.[60,147]

The paradox with M-N_x/C catalysts is that their synthesis also yields nitrogen-functionalized carbon species which are not coordinated to the metal.[143] Therefore, M-N_x/C catalysts do not exclusively contain only M-N_x/C-type active sites per se, but also contain active sites akin to NC-type catalysts. In this case, it becomes difficult to resolve the fraction of oxygen reduced on M-N_x/C sites and that reduced on NC-type sites. Most theories of the active sites of M-N_x/C and NC catalysts are based on deductions from ex situ physicochemical characterizations, including XPS, time of flight-secondary ion mass spectroscopy (TOF-SIMS), X-ray absorption spectroscopy (XAS) including XANES and EXAFS, Mössbauer spectrometry, XRD, Raman spectroscopy, transmission electron microscopy (TEM), scanning electron microscopy (SEM), Brunauer–Emmett–Teller (BET) surface area determination, and the degree of porosity. However, information acquired from ex situ measurements may not be of relevance in an electrochemical environment. In the case of the metal-free catalysts, although some studies report performance nearly as good as Pt or M-N_x/C-type catalysts in alkaline electrolytes, the physicochemical information available from standard characterization techniques does not provide conclusive evidence on why the same metal-free catalysts perform a lot worse than Pt and M-N_x/C catalysts in acidic electrolytes. One therefore recognizes that only in situ observations can provide reliable information about the nature of active sites and the mechanism of the ORR.

Direct observation of the involvement of the metal ions in M-N_x/C type catalysts as active centers during the ORR has been achieved with various in situ techniques including X-ray absorption spectroscopy,[121,143] Mössbauer spectroscopy,[45] and by electrochemical measurements.[121,166] For example, in a recent study, Mukerjee and co-workers[121] observed that oxygen reduction on Fe-N_x/C in H_2SO_4 (0.5 M) commences at a potential coinciding with the $Fe^{3+} \rightarrow Fe^{2+}$ redox transition, in excellent agreement with the redox-type mechanism proposed in Figure 6. More interestingly, the intensities of the Fe^{2+}/Fe^{3+} signal diminished when CN^- ions were introduced into the electrolyte and was accompanied by a concomitant decline in the ORR activity. These findings strongly support the theory of the direct involvement of metal ions as an essential part of the active sites. Iron is a very common impurity in many commercial products. It is usually introduced when these chemicals are synthesized in stainless-steel reactors. For example, perylenetetracarboxylic dianhydride was found to contain about 1600 ppm Fe, enough to influence the ORR when it was used as a carbon precursor in the synthesis of a metal-free NC catalyst.[167] As one would expect, metals or metal ions are electroactive and will naturally undergo redox transition or mediate in electrode reactions when the electrode is at a suitable potential. The extreme sensitivity of voltammetric responses on trace impurities of Fe was highlighted by Trotochaud et al.,[168] where the voltammetric features of a $Ni(OH)_2$/NiOOH redox couple varied considerably in the presence of less than 1 ppm Fe and produced a pronounced effect on the O_2 evolution activity of the electrode. XPS showed that Fe was incorporated within the $Ni(OH)_2$/NiOOH film. We observed a dramatic increase in ORR activity when as little of 0.05 wt% Fe was introduced in a metal-free NC

catalyst. These observations underpin the drastic effects that metal impurities can impart on voltammetric measurements.[47,48] To further highlight the influence of metal inclusions in NC catalysts, we present and discuss in Section 4.3 examples of poisoning tests by using specific anions as probes to mask and exclude the involvement of metal ions in the electrochemical reduction of oxygen.

4.3. ORR Poisoning Tests

The ability of Fe to coordinate specific anions has been utilized as a means to probe its involvement in the electrocatalytic reduction of O_2. According to the redox mechanism for O_2 reduction on M-N_x/C catalysts (Figure 6), the reduction of O_2 is expected to precede its adsorption on Fe^{2+}. The rationality of the poisoning test is that if another molecule or ion competitively binds on Fe^{2+}, it masks the coordination sites that would be otherwise available for the adsorption of O_2, thus inhibiting the ORR.

CN^- ions are known to readily coordinate with Fe. Yeager and co-workers[169] employed CN^- ions to probe the redox properties of cobalt and iron phthalocyanine as well as the involvement of the metal ions in the ORR in NaOH (0.1 M). A decrease or even complete disappearance of redox peaks characteristic of Co^{I}/Co^{II}, Co^{II}/Co^{III}, and Fe^{II}/Fe^{III} was observed in the presence of CN^- ions, concomitant with a drastic decline in the electrocatalytic current for ORR. A change in the mechanism from a four electron transfer pathway to a two electron pathway was also observed when NaCN (1.0 mM) was added to the electrolyte. In the case of cobalt tetramethoxyphenylporphyrin, the reduction of O_2 was inhibited by at least 120 mV in addition to a decline of the diffusion-limited current. Interestingly, the catalysts regained nearly their full activity upon rinsing, thus confirming that the metal ions were directly involved as active sites. More recently, Thorum et al.[141] observed diminished activity of iron phthalocyanine (FePc) in the presence of CN^-, thus suggesting that the CN^- ions compete with O_2 for the active sites (Figure 13).

The authors concluded that the active sites for the ORR in FePc, both before and after pyrolysis, were iron-centered. Several other anions and molecules have been investigated as possible poisoning agents, including CO, Br^-, Cl^-, F^-, SCN^-, H_2S, SO_2, and ethanethiol (EtSH).[141,142,170,171] Among these agents, CN^-, H_2S, and SCN^- show the best inhibitory effects and have been employed in other studies to demonstrate Fe-centered ORR electrocatalysis.[68,69,172] Liu et al.[68] also observed a decrease in the activity of an Fe-N_x/C catalyst when exposed to KCN. In similar studies, a poisoned Fe-based catalyst regained most of its activity after washing it in water before retesting the electrodes in clean electrolyte.[69] The Murkejee research group[121] also employed CN^- ions to probe Fe-centered activity in Fe-N_x/C catalysts. In their studies, the ORR was recorded first in the absence of CN^- and then in the presence of CN^- in KOH (0.1 M) and in $HClO_4$ (0.1 M). Significant increases in the overpotential for O_2 reduction and a decline in the catalytic current were observed in the presence of CN^- ions in both KOH and $HClO_4$.

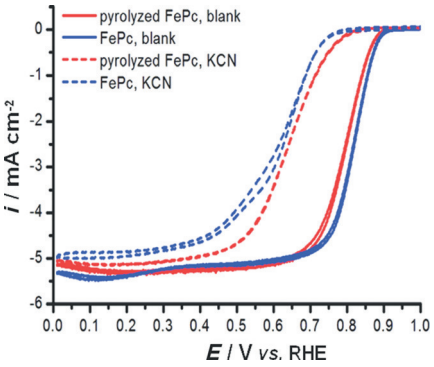

Figure 13. RDE measurements of O_2 reduction by carbon-supported FePc (blue lines) and pyrolyzed carbon-supported FePc (red lines) in O_2-saturated 0.1 M NaOH alone (solid lines) and containing 10 mM KCN. Reproduced from Ref. [141] with permission from the ACS.

RRDE results revealed that whereas the poisoning effect did not affect the mechanism of O_2 reduction in $HClO_4$ (0.1 M), there was an evident alteration in the mechanism in KOH (0.1 M) from a four to a two electron transfer process that led to considerable generation of H_2O_2.[121] The residual catalytic effect was attributed to the NC moieties, which are not expected to be poisoned by the CN^- ions. This study further confirms that NC sites predominantly reduce O_2 through the two electron transfer pathway to form H_2O_2.

The examples in Figure 14 show inhibition of Fe-centered electrocatalytic O_2 reduction when using SCN^- and H_2S as the poisoning agents. In Figure 14a, SCN^- ions were used to probe the involvement of Fe-containing moieties in a catalyst comprised of Fe-N_x/C and perovskites in the electrocatalytic reduction of O_2.[172] In this case, voltammograms were recorded in O_2-saturated 0.1 M KOH before and after immersing the electrode in KSCN (5.0 mM) for 1 h. Figure 14a shows a comparison of the ORR before and after exposure of the electrode to SCN^- ions. An increase in the overpotential of 50 mV at -4 mA cm^{-2} and a current loss of 0.5 mA cm^{-2} at 0.5 V were observed after the poisoning test, thereby indicating that Fe was directly involved in the electrocatalytic reduction of O_2. Since SCN^- ions can coordinate strongly on Fe^{II} and Fe^{III}, the decline in the current was attributed to lower availability of Fe-containing active sites.

Singh et al.[171] investigated the possibility of using H_2S as a poisoning agent to probe the active sites in Fe-N_x/C catalysts by using two approaches. In the first approach, a Fe-N_x/C catalyst was subjected to thermal treatment at 350 °C under an atmosphere of H_2S, and the effect of this treatment on the ORR was investigated by RDE voltammetry in H_2SO_4 (0.5 M). For comparison, the catalyst was also treated under similar conditions but in the presence of NH_3, H_2, and Ar. The sample treated under H_2S exhibited an overpotential of at least 30 mV higher for the ORR than the samples treated under NH_3 and Ar, thus indicating that the presence of H_2S poisoned the catalyst. In the second approach, H_2S (500 ppm) was introduced into the electrolyte by bubbling for at least 75 min. In comparison with the electrolyte free of H_2S, a net activity decline was observed, with a higher overpotential and lower catalytic current (Figure 14b) in the electrolyte con-

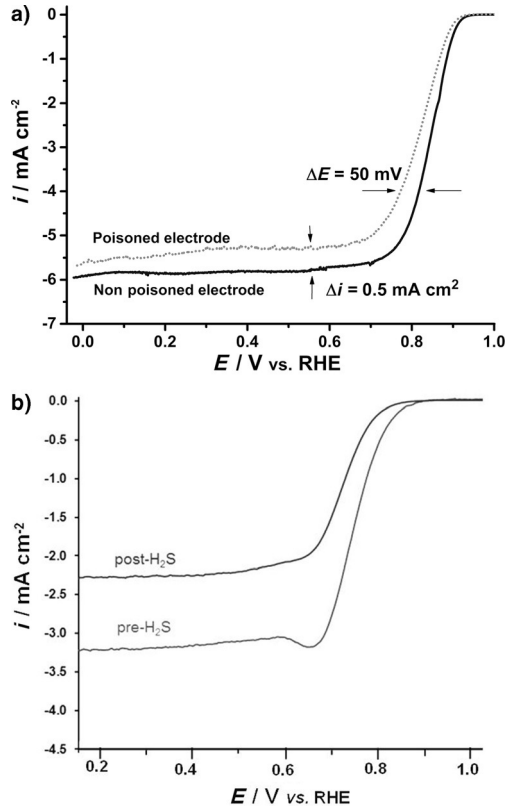

Figure 14. a) Background-corrected voltammogram recorded at 10 $mV s^{-1}$ with Fe-N_x/C/L58SCF before and after immersion of the electrode in 5 mM KSCN for 1 h, in O_2-saturated KOH (0.1 M) and at an electrode rotation of 2500 rpm. Reprinted from Ref. [172] with permission from the RSC. b) ORR activity measurements of FeNC-Ar-NH_3 by RDE in O_2-saturated 0.1 M $HClO_4$ before and after in situ exposure to H_2S at 500 ppm. Reprinted from Ref. [171] with permission from the ACS.

taining H_2S. The loss of activity was ascribed to blockage of the Fe-containing active sites because of the binding of H_2S to the metal.[171]

4.4. The Role of the Metals

By considering the examples discussed herein and other reports from the literature, we may conclude that the metal plays either a direct or an indirect role in M-N_x/C catalysts. It is important to bear in mind that if metal-free catalysts are synthesized using metal precursors (for example, as catalysts for CVD or as precursors during pyrolysis), they may contain metal residues that are difficult to remove completely. This is particularly true if the metal residues are encapsulated inside graphitic structures, or if they are stabilized in forms that make it difficult to leach them out using mineral acids.[67,103] Metal impurities in carbon materials can drastically affect electrochemical reactions.[70,173] For example, it was demonstrated that metal impurities within CNTs were responsible for the oxidation of hydrazine on CNTs,[76] while iron oxide residues from the synthesis of CNTs by CVD were shown to dominate the electrocatalytic detection of H_2O_2 on the CNTs.[74] The poisoning tests discussed in the preceding section provide unequivocal evidence of the involvement of metal ions in electrocatalyzing the ORR.

4.4.1. Direct Interaction

In this case, the metal is directly involved in the mediation of O_2 reduction as an active site, and its reduction takes place through the redox-type mechanism outlined in Figure 6. Poisoning studies using anions which specifically coordinate on Fe give conclusive evidence of the direct involvement of Fe in the active sites or in activating the active sites. Atannasov and co-workers[174] proposed dual active sites in Co-N_x/C catalysts, where the N-modified carbon moieties catalyze the reduction of O_2 to H_2O_2 while oxide-covered cobalt particles catalyze the decomposition of the formed H_2O_2.

4.4.2. Indirect Interaction

The indirect contribution of metals applies to the case where the metals do not directly interact with O_2 but where the electronic properties of the active sites in NC are modified by virtue of the presence of metal entities, as may be the case of metal particles encapsulated inside CNTs. The Bao research group[67] recently reported the synthesis of O_2 reduction catalysts with Fe encapsulated in peapod-like CNTs by subjecting a mixture of sodium azide and ferrocene to pyrolysis at 350 °C in N_2. The use of $(NH_4)_4[Fe(CN)_6]\cdot x\,H_2O$ instead of ferrocene as an iron precursor led to an enhancement in activity, which was ascribed to functionalization of the active sites with nitrogen. Poisoning tests using CN^- ions did not affect the ORR activity, thus leading the authors to conclude that Fe promotes the ORR without directly interacting with it. Some studies thus suggest that metals only promote the formation of graphitic nitrogen and a high degree of sp^2-hybridized carbon necessary for ensuring high electrical conductivity.[61,148,175] One may argue that if this is to be true, a theory would be required to explain why Fe- and Co-containing M-N_x/C catalysts and not Ni, Mn, and Mo tend to yield catalysts with the highest ORR activity. Peng et al.[162] proposed that metals are involved in a variety of functions, including catalyzing the formation of NC structures, regulating the morphology, surface area, and pore structure of the NC catalyst, and participation of the metal residues in the ORR.

4.4.3. Utilization of Residual Metals for Electrocatalysis

Metal residues encapsulated in CNTs can be exposed and utilized for electrocatalysis. In a recent study, we synthesized NCNTs by chemical vapor deposition using spinel-type cobalt-manganese-based mixed oxides as the growth catalyst and pyridine as the nitrogen and carbon precursor. After washing the NCNTs with HNO_3 to remove surface-exposed residual metal particles, encapsulated metal residues inside the NCNT were exposed by oxidative thermal scission with simultaneous oxidation, thereby leading to formation of partially exposed metal oxides embedded in the CNTs. The resulting materials were highly active for both O_2 reduction and O_2 evolution.[80] Recently, Bao and co-workers[84] reported the synthesis of NCNTs encapsulating Fe, Co, and

FeCo nanoparticles by controlled exposure of the metals and demonstrated their application as very active electrocatalysts for the hydrogen evolution reaction in acidic electrolytes. In a related study, Deng et al.[67] developed a very active and stable O_2 reduction catalyst comprised of Fe particles encapsulated inside CNTs. Li et al.[69] unzipped MWCNTs to expose Fe, and by a further treatment step with NH_3, they were able to transform them into a very active and stable catalyst for O_2 reduction under both acidic and alkaline conditions. To probe whether Fe was involved in the active sites, the authors added CN^- ions to the electrolyte and observed a degeneration of activity, thus suggesting that Fe was directly involved as part of the active site(s). In related studies, it was demonstrated that metal impurities intercalated within the graphene lattice of CNTs were chemically accessible and participated in the redox chemistry of biomarkers by intercalation of molecules within the CNT lattice.[163]

5. Stability of M-N_x/C and NC Catalysts

M-N_x/C catalysts are top contenders among non-platinum O_2 reduction catalysts.[89,91,103,107] Their greatest drawback, which has hampered commercial deployment, is the rapid decay of their activity, especially in acidic electrolytes. The longest stability tests of M-N_x/C in fuel cells have lasted only a few hundred hours, thus falling far short of the DOE target of at least 5000 h.[117] Moreover, most of these tests are often performed at much lower cell voltages, typically 0.3–0.5 V.[103,107,156,176] For example, a hydrogen/air fuel cell (PEM) operating at 0.6 V with Fe-PANI/C as the cathode and JM-Pt/C as the anode lost over 75% of its activity within 10 h.[105] On the other hand, fuel cells with Fe-PANI/C or Co-PANI/C as cathodes and Pt/C as the anode and running at 0.4 V were able to sustain relatively stable performances for only about 200 h.[103] Future research on M-N_x/C should focus on strategies for improving the stability of the catalysts.[57] Some recent and promising strategies for stabilization of M-N_x/C-type-catalysts include partial[69] or complete encapsulation of the metals in CNTs[67,84] or in graphitic layers to protect them from acidic attack. A H_2/O_2 fuel cell operating on Fe encapsulated within podlike CNTs as the cathode and Pt/C (JM) as the anode sustained relatively stable performance for at least 200 h at a cell voltage of about 0.40 V.[67]

Stability tests on metal-free NC catalysts in fuel cells have rarely been reported. Most stability tests are based on simple potentiostatic or galvanostastic tests in three-electrode electrochemical cells.[38,126,157] A fuel cell based on an anion-exchange membrane using nitrogen-doped CNTs as the cathode and Pt/C as the anode delivered a stable current of 20 mA cm^{-2} for 30 h at a cell voltage of 0.65 V.[176] This cell voltage was, however, about 120 mV lower than a similar cell using a Pt/C cathode at the same current density. NC catalysts, however, demonstrate very stable performance in Zn/air batteries, with a performance rivaling that of platinum.[131,140,160]

Unlike the M-N_x/C catalysts, whose performance decline when they lose their metal ions, the degradation mechanisms of NC catalysts are not well understood yet. However, it is expected that fuel cells using NC catalysts as the cathode catalyst should experience detrimental effects from H_2O_2, if this is formed during the ORR. Future efforts should, therefore, focus more on testing NC catalysts in real fuel cells so that more about their performance and stability can be understood.

6. Summary and Outlook

Metal-free heteroatom-doped carbon catalysts have emerged as a competitive class of nonprecious-metal catalysts for the ORR. In particular, metal-free NC catalysts offer very positive prospects of replacing the costly precious-metal-based catalysts that are currently used in fuel cells and in chlor-alkali electrolyzers, thereby leading to a significant reduction in the cost of their operation. Remarkable progress has been achieved in the development of metal-free NC catalysts for the ORR over the past decade, driven by better understanding of their property–activity relationships. However, some reported metal-free NC catalysts are prepared using metal precursors, mostly as catalysts to facilitate the formation of NC structures. The metal residues have to be later removed by leaching with mineral acids. However, complete removal of the metal residues may not be possible, especially if the residual metal particles are encapsulated inside graphitic layers, as in the case of CNTs. There is profound concern that metal residues in NC catalysts at concentrations which may not be detectable using common analytical techniques may significantly influence the ORR.

Metal-free NC catalysts generally show reasonable activity for the ORR in both acidic and alkaline electrolytes. However, the ORR activity of truly metal-free NC catalysts in acidic electrolytes is a lot lower than that of M-N_x/C or Pt/C catalysts. Metal-free NC catalysts reduce O_2 through a two electron transfer pathway to form H_2O_2 in acidic electrolytes. However, there is widespread disharmony in the literature, both from experimental and theoretical perspectives, on the mechanism of the ORR on NC catalysts, with some claiming direct four-electron reduction while others report two-electron reduction of O_2. Part of this conflict is caused by the wide variation of activity parameters, which include the nature of the predominant active sites and their density of distribution, the active surface area of the catalyst, and the degrees of porosity and graphitization. It is important to mention that the inconsistency regarding the selectivity of the ORR is also partly due to variations in experimental standards across laboratories and from the shortcomings of applying the Koutecky–Levich method when studying the mechanism of the ORR on highly dispersed and heterogeneous electrode surfaces.

In general, M-N_x/C catalysts are more active than NC catalysts in both acidic and alkaline electrolytes. The synthesis of M-N_x/C catalysts also generates NC moieties. M-N_x/C catalysts, therefore, comprise an ensemble of heterogeneous active sites whose intrinsic activities for O_2 reduction spread over a range of potentials. It is, therefore, difficult to distinguish between the fraction of O_2 reduced on M-N_x/C

sites and that reduced on NC sites. However, in situ XAS and poisoning tests unequivocally show that metal ions are directly involved in mediating the ORR on M-N_x/C catalysts. Inhibition of M-N_x/C sites using a suitable poisoning agent can alter the mechanism of O_2 reduction from a four-electron transfer process to a two-electron transfer process in 0.1 M KOH.

Most theories on the active sites of M-N_x/C and NC catalysts are based on ex situ physicochemical characterization. However, such information may not necessarily be relevant or valid under real electrochemical conditions. It is, therefore, highly desirable to see more effort devoted towards in situ as well as in operando studies to gain a deeper understanding on the true nature of active sites of both NC and M-N_x/C catalysts. This will be indispensable to understand the nature of the intrinsically most active sites, M-N_x/C or NC, so that future efforts are directed towards maximizing their density in an effort to design advanced nonprecious-metal catalysts for the ORR.

There is sufficient evidence that residual metals, specifically Fe, even at trace levels undetectable by XPS and EDX, promote the ORR. Therefore, in cases where the preparation of the NC catalysts involves the use of metals, it is instructive to employ ultrasensitive methods of metal analysis—including ICP-OES, magnetic susceptibility, AAS, and NAA—which offer much lower detection limits for most metals. Nevertheless, we urge that the designation of metal-free catalysts be reserved for catalysts prepared without the involvement of any metallic precursors, or if they are prepared using metal precursors there ought to be definitive proof of the absence of metal residues in the catalysts.

The widespread discrepancy between experimental results on metal-free NC catalysts and their interpretation can only be solved through more careful experimentation and rigorous treatment of RDE and RRDE data. Finally, after at least 10 years of intensive fundamental investigation and development, the ultimate viability test of metal-free catalysts should be their investigation in real fuel cell prototypes. We, therefore, advocate that future research efforts on metal-free NC catalysts for the ORR focus more on their investigation in fuel cells—a step towards real applications.

Financial support from the DFG in the framework of the Cluster of Excellence RESOLV (EXC1069), the Helmholtz-Energie-Allianz "Stationäre elektrochemische Speicher und Wandler" (HA-E-0002), and the BMBF "Sustainable Hydrogen (SusHy)" (03X3581D) is gratefully acknowledged.

How to cite: *Angew. Chem. Int. Ed.* **2015**, *54*, 10102 – 10120
Angew. Chem. **2015**, *127*, 10240 – 10259

[1] M. Zhang, L. Dai, *Nano Energy* **2012**, *1*, 514 – 517.
[2] D. Yu, E. Nagelli, F. Du, L. Dai, *J. Phys. Chem. Lett.* **2010**, *1*, 2165 – 2173.
[3] Y. Zheng, Y. Jiao, M. Jaroniec, Y. Jin, S. Z. Qiao, *Small* **2012**, *8*, 3550 – 3566.
[4] S. Wang, L. Zhang, Z. Xia, A. Roy, D. W. Chang, J.-B. Baek, L. Dai, *Angew. Chem. Int. Ed.* **2012**, *51*, 4209 – 4212; *Angew. Chem.* **2012**, *124*, 4285 – 4288.
[5] L. Yang, Y. Zhao, S. Chen, Q. Wu, X. Wang, Z. Hu, *Chin. J. Catal.* **2013**, *34*, 1986 – 1991.
[6] R. Liu, D. Wu, X. Feng, K. Müllen, *Angew. Chem. Int. Ed.* **2010**, *49*, 2565 – 2569; *Angew. Chem.* **2010**, *122*, 2619 – 2623.
[7] H. Shi, Y. Shen, F. He, Y. Li, A. Liu, S. Liu, Y. Zhang, *J. Mater. Chem. A* **2014**, *2*, 15704 – 15716.
[8] N. Daems, X. Sheng, I. F. J. Vankelecom, P. P. Pescarmona, *J. Mater. Chem. A* **2014**, *2*, 4085 – 4110.
[9] Z. Yang, H. Nie, X. Chen, X. Chen, S. Huang, *J. Power Sources* **2013**, *236*, 238 – 249.
[10] D. S. Su, J. Zhang, B. Frank, A. Thomas, X. Wang, J. P. Paraknowitsch, R. Schlögl, *ChemSusChem* **2010**, *3*, 169 – 180.
[11] O. Stephan, P. M. Ajayan, C. Colliex, P. Redlich, J. M. Lambert, P. Bernier, P. Lefin, *Science* **1994**, *266*, 1683 – 1685.
[12] H. Wang, T. Maiyalagan, X. Wang, *ACS Catal.* **2012**, *2*, 781 – 794.
[13] L. S. Panchakarla, K. S. Subrahmanyam, S. K. Saha, A. Govindaraj, H. R. Krishnamurthy, U. V. Waghmare, C. N. R. Rao, *Adv. Mater.* **2009**, *21*, 4726 – 4730.
[14] P. Ayala, R. Arenal, M. Ruemmeli, A. Rubio, T. Pichler, *Carbon* **2010**, *48*, 575 – 586.
[15] K. Gong, F. Du, Z. Xia, M. Durstock, L. Dai, *Science* **2009**, *323*, 760 – 764.
[16] C. H. Choi, S. H. Park, S. I. Woo, *ACS Nano* **2012**, *6*, 7084 – 7091.
[17] Y. Zheng, Y. Jiao, L. Ge, M. Jaroniec, S. Z. Qiao, *Angew. Chem. Int. Ed.* **2013**, *52*, 3110 – 3116; *Angew. Chem.* **2013**, *125*, 3192 – 3198.
[18] W. Xia, J. Masa, M. Bron, W. Schuhmann, M. Muhler, *Electrochem. Commun.* **2011**, *13*, 593 – 596.
[19] G. Liu, X. Li, J.-W. Lee, B. N. Popov, *Catal. Sci. Technol.* **2011**, *1*, 207 – 217.
[20] W. Y. Wong, W. Daud, A. B. Mohamad, A. Kadhum, K. S. Loh, E. H. Majlan, *Int. J. Hydrogen Energy* **2013**, *38*, 9370 – 9386.
[21] K. N. Wood, R. O'Hayre, S. Pylypenko, *Energy Environ. Sci.* **2014**, *7*, 1212 – 1249.
[22] L. Qu, Y. Liu, J.-B. Baek, L. Dai, *ACS Nano* **2010**, *4*, 1321 – 1326.
[23] Z.-W. Liu, F. Peng, H.-J. Wang, H. Yu, W.-X. Zheng, J. Yang, *Angew. Chem. Int. Ed.* **2011**, *50*, 3257 – 3261; *Angew. Chem.* **2011**, *123*, 3315 – 3319.
[24] R. Liu, H. Liu, Y. Li, Y. Yi, X. Shang, S. Zhang, X. Yu, S. Zhang, H. Cao, G. Zhang, *Nanoscale* **2014**, *6*, 11336 – 11343.
[25] S. Yang, X. Feng, X. Wang, K. Müllen, *Angew. Chem. Int. Ed.* **2011**, *50*, 5339 – 5343; *Angew. Chem.* **2011**, *123*, 5451 – 5455.
[26] Y. Tang, B. L. Allen, D. R. Kauffman, A. Star, *J. Am. Chem. Soc.* **2009**, *131*, 13200 – 13201.
[27] T. Ikeda, M. Boero, S.-F. Huang, K. Terakura, M. Oshima, J.-i. Ozaki, *J. Phys. Chem. C* **2008**, *112*, 14706 – 14709.
[28] Y. Zhao, L. Yang, S. Chen, X. Wang, Y. Ma, Q. Wu, Y. Jiang, W. Qian, Z. Hu, *J. Am. Chem. Soc.* **2013**, *135*, 1201 – 1204.
[29] W. Wei, H. Liang, K. Parvez, X. Zhuang, X. Feng, K. Müllen, *Angew. Chem. Int. Ed.* **2014**, *53*, 1570 – 1574; *Angew. Chem.* **2014**, *126*, 1596 – 1600.
[30] L. Yang, S. Jiang, Y. Zhao, L. Zhu, S. Chen, X. Wang, Q. Wu, J. Ma, Y. Ma, Z. Hu, *Angew. Chem. Int. Ed.* **2011**, *50*, 7132 – 7135; *Angew. Chem.* **2011**, *123*, 7270 – 7273.
[31] a) X. Sun, Y. Zhang, P. Song, J. Pan, L. Zhuang, W. Xu, W. Xing, *ACS Catal.* **2013**, *3*, 1726 – 1729; b) X. Sun, P. Song, T. Chen, J. Liu, W. Xu, *Chem. Commun.* **2013**, *49*, 10296 – 10298; c) H. Wang, A. Kong, *Mater. Lett.* **2014**, *136*, 384 – 387.
[32] L. Lai, J. R. Potts, D. Zhan, L. Wang, C. K. Poh, C. Tang, H. Gong, Z. Shen, J. Lin, R. S. Ruoff, *Energy Environ. Sci.* **2012**, *5*, 7936 – 7942.
[33] a) J. Wu, Z. Yang, Q. Sun, X. Li, P. Strasser, R. Yang, *Electrochim. Acta* **2014**, *127*, 53 – 60; b) D.-S. Yang, D. Bhattacharjya, S. Inamdar, J. Park, J.-S. Yu, *J. Am. Chem. Soc.* **2012**,

134, 16127 – 16130; c) J. Wu, C. Jin, Z. Yang, J. Tian, R. Yang, *Carbon* **2015**, *82*, 562 – 571.
[34] Y. Meng, D. Voiry, A. Goswami, X. Zou, X. Huang, M. Chhowalla, Z. Liu, T. Asefa, *J. Am. Chem. Soc.* **2014**, *136*, 13554 – 13557.
[35] a) Z. Yang, Z. Yao, G. Li, G. Fang, H. Nie, Z. Liu, X. Zhou, X. Chen, S. Huang, *ACS Nano* **2012**, *6*, 205 – 211; b) Z. Ma, S. Dou, A. Shen, L. Tao, L. Dai, S. Wang, *Angew. Chem. Int. Ed.* **2015**, *54*, 1888 – 1892; *Angew. Chem.* **2015**, *127*, 1908 – 1912.
[36] R. A. Sidik, A. B. Anderson, N. P. Subramanian, S. P. Kumaraguru, B. N. Popov, *J. Phys. Chem. B* **2006**, *110*, 1787 – 1793.
[37] H. Kim, K. Lee, S. I. Woo, Y. Jung, *Phys. Chem. Chem. Phys.* **2011**, *13*, 17505 – 17510.
[38] C. V. Rao, C. R. Cabrera, Y. Ishikawa, *J. Phys. Chem. Lett.* **2010**, *1*, 2622 – 2627.
[39] a) T. Xing, Y. Zheng, L. H. Li, B. C. C. Cowie, D. Gunzelmann, S. Z. Qiao, S. Huang, Y. Chen, *ACS Nano* **2014**, *8*, 6856 – 6862; b) S.-F. Huang, K. Terakura, T. Ozaki, T. Ikeda, M. Boero, M. Oshima, J.-i. Ozaki, S. Miyata, *Phys. Rev. B* **2009**, *80*, 235410; c) B. Zhang, Z. Wen, S. Ci, S. Mao, J. Chen, Z. He, *ACS Appl. Mater. Interfaces* **2014**, *6*, 7464 – 7470.
[40] a) K. A. Kurak, A. B. Anderson, *J. Phys. Chem. C* **2009**, *113*, 6730 – 6734; b) N. P. Subramanian, X. Li, V. Nallathambi, S. P. Kumaraguru, H. Colon-Mercado, G. Wu, J.-W. Lee, B. N. Popov, *J. Power Sources* **2009**, *188*, 38 – 44; c) T. C. Nagaiah, S. Kundu, M. Bron, M. Muhler, W. Schuhmann, *Electrochem. Commun.* **2010**, *12*, 338 – 341.
[41] A. Zhao, J. Masa, M. Muhler, W. Schuhmann, W. Xia, *Electrochim. Acta* **2013**, *98*, 139 – 145.
[42] S. Kundu, T. C. Nagaiah, W. Xia, Y. Wang, S. van Dommele, J. H. Bitter, M. Santa, G. Grundmeier, M. Bron, W. Schuhmann, M. Muhler, *J. Phys. Chem. C* **2009**, *113*, 14302 – 14310.
[43] Y. Okamoto, *Appl. Surf. Sci.* **2009**, *256*, 335 – 341.
[44] T. Sharifi, G. Hu, X. Jia, T. Wågberg, *ACS Nano* **2012**, *6*, 8904 – 8912.
[45] A. L. Bouwkamp-Wijnoltz, W. Visscher, J. A. R. van Veen, E. Boellaard, A. M. van der Kraan, S. C. Tang, *J. Phys. Chem. B* **2002**, *106*, 12993 – 13001.
[46] S. Liu, C. Deng, L. Yao, H. Zhong, H. Zhang, *J. Power Sources* **2014**, *269*, 225 – 235.
[47] J. Masa, A. Zhao, W. Xia, Z. Sun, B. Mei, M. Muhler, W. Schuhmann, *Electrochem. Commun.* **2013**, *34*, 113 – 116.
[48] J. Masa, A. Zhao, W. Xia, M. Muhler, W. Schuhmann, *Electrochim. Acta* **2014**, *128*, 271 – 278.
[49] J. P. Dodelet, *Lecture Notes in Energy* (Ed.: M. Shao), Springer, London, **2013**.
[50] a) Z. Shi, H. Liu, K. Lee, E. Dy, J. Chlistunoff, M. Blair, P. Zelenay, J. Zhang, Z.-S. Liu, *J. Phys. Chem. C* **2011**, *115*, 16672 – 16680; b) T. Schilling, A. O. Okunola, J. Masa, W. Schuhmann, M. Bron, *Electrochim. Acta* **2010**, *55*, 7597 – 7602.
[51] F. Jaouen, M. Lefevre, J. P. Dodelet, M. Cai, *J. Phys. Chem. B* **2006**, *110*, 5553 – 5558.
[52] F. Jaouen, J. P. Dodelet, *J. Phys. Chem. C* **2009**, *113*, 15422 – 15432.
[53] H. Tributsch, U. I. Koslowski, I. Dorbandt, *Electrochim. Acta* **2008**, *53*, 2198 – 2209.
[54] G. Faubert, R. Côté, D. Guay, J. P. Dodelet, G. Denes, C. Poleunis, P. Bertrand, *Electrochim. Acta* **1998**, *43*, 1969 – 1984.
[55] G. Lalande, R. Côté, D. Guay, J. P. Dodelet, L. T. Weng, P. Bertrand, *Electrochim. Acta* **1997**, *42*, 1379 – 1388.
[56] M. Lefèvre, J. P. Dodelet, P. Bertrand, *J. Phys. Chem. B* **2000**, *104*, 11238 – 11247.
[57] F. Jaouen, E. Proietti, M. Lefevre, R. Chenitz, J. P. Dodelet, G. Wu, H. T. Chung, C. M. Johnston, P. Zelenay, *Energy Environ. Sci.* **2011**, *4*, 114 – 130.
[58] F. Jaouen, J. Herranz, M. Lefèvre, J. P. Dodelet, U. I. Kramm, I. Herrmann, P. Bogdanoff, J. Maruyama, T. Nagaoka, A. Garsuch, J. R. Dahn, T. Olson, S. Pylypenko, P. Atanassov, E. A. Ustinov, *ACS Appl. Mater. Interfaces* **2009**, *1*, 1623 – 1639.
[59] M. Ladouceur, *J. Electrochem. Soc.* **1993**, *140*, 1974 – 1981.
[60] H. Wang, R. Côté, G. Faubert, D. Guay, J. P. Dodelet, *J. Phys. Chem. B* **1999**, *103*, 2042 – 2049.
[61] P. H. Matter, E. Wang, M. Arias, E. J. Biddinger, U. S. Ozkan, *J. Phys. Chem. B* **2006**, *110*, 18374 – 18384.
[62] M. Kobayashi, H. Niwa, Y. Harada, K. Horiba, M. Oshima, H. Ofuchi, K. Terakura, T. Ikeda, Y. Koshigoe, J.-i. Ozaki, S. Miyata, S. Ueda, Y. Yamashita, H. Yoshikawa, K. Kobayashi, *J. Power Sources* **2011**, *196*, 8346 – 8351.
[63] C. H. Choi, H.-K. Lim, M. W. Chung, J. C. Park, H. Shin, H. Kim, S. I. Woo, *J. Am. Chem. Soc.* **2014**, *136*, 9070 – 9077.
[64] M. Kobayashi, H. Niwa, M. Saito, Y. Harada, M. Oshima, H. Ofuchi, K. Terakura, T. Ikeda, Y. Koshigoe, J.-i. Ozaki, S. Miyata, *Electrochim. Acta* **2012**, *74*, 254 – 259.
[65] Y. Tang, S. C. Burkert, Y. Zhao, W. A. Saidi, A. Star, *J. Phys. Chem. C* **2013**, *117*, 25213 – 25221.
[66] D. Singh, J. Tian, K. Mamtani, J. King, J. T. Miller, U. S. Ozkan, *J. Catal.* **2014**, *317*, 30 – 43.
[67] D. Deng, L. Yu, X. Chen, G. Wang, L. Jin, X. Pan, J. Deng, G. Sun, X. Bao, *Angew. Chem. Int. Ed.* **2013**, *52*, 371 – 375; *Angew. Chem.* **2013**, *125*, 389 – 393.
[68] J. Liu, X. Sun, P. Song, Y. Zhang, W. Xing, W. Xu, *Adv. Mater.* **2013**, *25*, 6879 – 6883.
[69] Y. Li, W. Zhou, H. Wang, L. Xie, Y. Liang, F. Wei, J.-C. Idrobo, S. J. Pennycook, H. Dai, *Nat. Nanotechnol.* **2012**, *7*, 394 – 400.
[70] C. E. Banks, A. Crossley, C. Salter, S. J. Wilkins, R. G. Compton, *Angew. Chem. Int. Ed.* **2006**, *45*, 2533 – 2537; *Angew. Chem.* **2006**, *118*, 2595 – 2599.
[71] L. Wang, M. Pumera, *Chem. Commun.* **2014**, *50*, 12662 – 12664.
[72] L. Wang, A. Ambrosi, M. Pumera, *Angew. Chem. Int. Ed.* **2013**, *52*, 13818 – 13821; *Angew. Chem.* **2013**, *125*, 14063 – 14066.
[73] X. Wang, H. Fu, W. Li, J. Zheng, X. Li, *RSC Adv.* **2014**, *4*, 37779.
[74] B. Šljukić, C. E. Banks, R. G. Compton, *Nano Lett.* **2006**, *6*, 1556 – 1558.
[75] M. Pumera, H. Iwai, *Chem. Asian J.* **2009**, *4*, 554 – 560.
[76] M. Pumera, H. Iwai, *J. Phys. Chem. C* **2009**, *113*, 4401 – 4405.
[77] T. Kolodiazhnyi, M. Pumera, *Small* **2008**, *4*, 1476 – 1484.
[78] K. Jurkschat, X. Ji, A. Crossley, R. G. Compton, C. E. Banks, *Analyst* **2007**, *132*, 21 – 23.
[79] M. Pumera, *Langmuir* **2007**, *23*, 6453 – 6458.
[80] A. Zhao, J. Masa, W. Xia, A. Maljusch, M.-G. Willinger, G. Clavel, K. Xie, R. Schlögl, W. Schuhmann, M. Muhler, *J. Am. Chem. Soc.* **2014**, *136*, 7551 – 7554.
[81] a) C. K. Chua, A. Ambrosi, Z. Sofer, A. Macková, V. Havránek, I. Tomandl, M. Pumera, *Chemistry* **2014**, *20*, 15760 – 15767; b) A. Ambrosi, M. Pumera, *Nanoscale* **2014**, *6*, 472 – 476; c) Z.-H. Sheng, L. Shao, J.-J. Chen, W.-J. Bao, F.-B. Wang, X.-H. Xia, *ACS Nano* **2011**, *5*, 4350 – 4358.
[82] A. Ambrosi, C. K. Chua, B. Khezri, Z. Sofer, R. D. Webster, M. Pumera, *Proc. Natl. Acad. Sci. USA* **2012**, *109*, 12899 – 12904.
[83] M. Pumera, Y. Miyahara, *Nanoscale* **2009**, *1*, 260 – 265.
[84] J. Deng, P. Ren, D. Deng, L. Yu, F. Yang, X. Bao, *Energy Environ. Sci.* **2014**, *7*, 1919 – 1923.
[85] J. Collman, P. Denisevich, Y. Konai, M. Marrocco, C. Koval, F. C. Anson, *J. Am. Chem. Soc.* **1980**, *102*, 6027 – 6036.
[86] E. Yeager, *Electrochim. Acta* **1984**, *29*, 1527 – 1537.
[87] L. Pauling, *Nature* **1964**, *203*, 182 – 183.
[88] J. S. Griffith, *Proc. R. Soc. London Ser. A* **1956**, *235*, 23 – 36.
[89] H. A. Gasteiger, S. S. Kocha, B. Sompalli, F. T. Wagner, *Appl. Catal. B* **2005**, *56*, 9 – 35.
[90] M. Koper, *Chem. Sci.* **2013**, *4*, 2710 – 2723.
[91] H. A. Gasteiger, N. M. Markovic, *Science* **2009**, *324*, 48 – 49.
[92] B. Wang, *J. Power Sources* **2005**, *152*, 1 – 15.
[93] a) V. Stamenkovic, B. S. Mun, K. J. J. Mayrhofer, P. N. Ross, N. M. Markovic, J. Rossmeisl, J. Greeley, J. K. Nørskov, *Angew.*

Chem. Int. Ed. **2006**, *45*, 2897 – 2901; *Angew. Chem.* **2006**, *118*, 2963 – 2967; b) V. R. Stamenkovic, B. S. Mun, M. Arenz, K. J. J. Mayrhofer, C. A. Lucas, G. Wang, P. N. Ross, N. M. Markovic, *Nat. Mater.* **2007**, *6*, 241 – 247; c) Z. Sun, J. Masa, W. Xia, D. König, A. Ludwig, Z.-A. Li, M. Farle, W. Schuhmann, M. Muhler, *ACS Catal.* **2012**, *2*, 1647 – 1653.

[94] I. Katsounaros, S. Cherevko, A. R. Zeradjanin, K. J. J. Mayrhofer, *Angew. Chem. Int. Ed.* **2014**, *53*, 102 – 121; *Angew. Chem.* **2014**, *126*, 104 – 124.

[95] Z. Chen, D. Higgins, A. Yu, L. Zhang, J. Zhang, *Energy Environ. Sci.* **2011**, *4*, 3167 – 3192.

[96] R. Jasinski, *Nature* **1964**, *201*, 1212 – 1213.

[97] a) V. Bagotzky, M. Tarasevich, K. Radyushkina, O. Levina, S. Andrusyova, *J. Power Sources* **1978**, *2*, 233 – 240; b) K. Wiesener, D. Ohms, V. Neumann, R. Franke, *Mater. Chem. Phys.* **1989**, *22*, 457 – 475.

[98] J. A. van Veen, J. F. VanBaar, K. J. Kroese, *J. Chem. Soc. Faraday Trans.* **1981**, *77*, 2827 – 2843.

[99] T. Okada, M. Gokita, M. Yuasa, I. Sekine, *J. Electrochem. Soc.* **1998**, *145*, 815 – 822.

[100] a) H. R. Byon, J. Suntivich, Y. Shao-Horn, *Chem. Mater.* **2011**, *23*, 3421 – 3428; b) C. W. B. Bezerra, L. Zhang, K. Lee, H. Liu, A. L. B. Marques, E. P. Marques, H. Wang, J. Zhang, *Electrochim. Acta* **2008**, *53*, 4937 – 4951.

[101] S. Gupta, D. Tryk, I. Bae, W. Aldred, E. Yeager, *J. Appl. Electrochem.* **1989**, *19*, 19 – 27.

[102] K. Kamiya, K. Hashimoto, S. Nakanishi, *Chem. Commun.* **2012**, *48*, 10213 – 10215.

[103] G. Wu, K. L. More, C. M. Johnston, P. Zelenay, *Science* **2011**, *332*, 443 – 447.

[104] a) J. Suntivich, H. A. Gasteiger, N. Yabuuchi, H. Nakanishi, J. B. Goodenough, Y. Shao-Horn, *Nat. Chem.* **2011**, *3*, 546 – 550; b) *Lecture Notes in Energy* (Ed.: M. Shao), Springer, London, **2013**.

[105] H. Peng, Z. Mo, S. Liao, H. Liang, L. Yang, F. Luo, H. Song, Y. Zhong, B. Zhang, *Sci. Rep.* **2013**, *3*, 1765.

[106] W. He, C. Jiang, J. Wang, L. Lu, *Angew. Chem. Int. Ed.* **2014**, *53*, 9503 – 9507; *Angew. Chem.* **2014**, *126*, 9657 – 9661.

[107] M. Lefevre, E. Proietti, F. Jaouen, J. P. Dodelet, *Science* **2009**, *324*, 71 – 74.

[108] A. Garsuch, A. Bonakdarpour, G. Liu, R. Yang, J. R. Dahn, *Time to move beyond transition metal - N - C catalysts for oxygen reduction*, Wiley, New York, **2010**.

[109] N. Ranjbar Sahraie, J. P. Paraknowitsch, C. Göbel, A. Thomas, P. Strasser, *J. Am. Chem. Soc.* **2014**, *136*, 14486 – 14497.

[110] J. van Veen, H. Colijn, J. van Baar, *Electrochim. Acta* **1988**, *33*, 801 – 804.

[111] M. Bron, J. Radnik, M. Fieber-Erdmann, P. Bogdanoff, S. Fiechter, *J. Electroanal. Chem.* **2002**, *535*, 113 – 119.

[112] T. S. Olson, S. Pylypenko, P. Atanassov, K. Asazawa, K. Yamada, H. Tanaka, *J. Phys. Chem. C* **2010**, *114*, 5049 – 5059.

[113] D. Scherson, A. Tanaka, S. Gupta, D. Tryk, C. Fierro, R. Holze, E. Yeager, R. Lattimer, *Electrochim. Acta* **1986**, *31*, 1247 – 1258.

[114] K. Wiesener, *Electrochim. Acta* **1986**, *31*, 1073 – 1078.

[115] M. Lefèvre, J. P. Dodelet, P. Bertrand, *J. Phys. Chem. B* **2002**, *106*, 8705 – 8713.

[116] Department of Energy (DOE) Fuel Cells technical plan section of the Fuel Cell Technologies Office Multi-Year Research, Development, and Demonstration (MYRD&D) Plan, updated November 2014. http://energy.gov/sites/prod/files/2014/12/f19/fcto_myrdd fuel cells.pdf.

[117] M. K. Debe, *Nature* **2012**, *486*, 43 – 51.

[118] E. Proietti, F. Jaouen, M. Lefèvre, N. Larouche, J. Tian, J. Herranz, J. P. Dodelet, *Nat. Commun.* **2011**, *2*, 416.

[119] a) R. Boulatov, J. Collman, I. M. Shiryaeva, C. J. Sunderland, *J. Am. Chem. Soc.* **2002**, *124*, 11923 – 11935; b) F. Beck, *J. Appl. Electrochem.* **1977**, *7*, 239 – 245.

[120] A. B. Anderson, R. A. Sidik, *J. Phys. Chem. B* **2004**, *108*, 5031 – 5035.

[121] U. Tylus, Q. Jia, K. Strickland, N. Ramaswamy, A. Serov, P. Atanassov, S. Mukerjee, *J. Phys. Chem. C* **2014**, *118*, 8999 – 9008.

[122] a) D. Higgins, M. A. Hoque, F. Hassan, J.-Y. Choi, B. Kim, Z. Chen, *ACS Catal.* **2014**, *4*, 2734 – 2740; b) H. Fei, R. Ye, G. Ye, Y. Gong, Z. Peng, X. Fan, E. L. G. Samuel, P. M. Ajayan, J. M. Tour, *ACS Nano* **2014**, *8*, 10837 – 10843; c) C. Han, X. Bo, Y. Zhang, M. Li, L. Guo, *J. Power Sources* **2014**, *272*, 267 – 276; d) S. Zhong, L. Zhou, L. Wu, L. Tang, Q. He, J. Ahmed, *J. Power Sources* **2014**, *272*, 344 – 350; e) S. Wang, E. Iyyamperumal, A. Roy, Y. Xue, D. Yu, L. Dai, *Angew. Chem. Int. Ed.* **2011**, *50*, 11756 – 11760; *Angew. Chem.* **2011**, *123*, 11960 – 11964; f) S. Zhao, J. Liu, C. Li, W. Ji, M. Yang, H. Huang, Y. Liu, Z. Kang, *ACS Appl. Mater. Interfaces* **2014**, *6*, 22297 – 22304; g) J. P. Paraknowitsch, A. Thomas, *Energy Environ. Sci.* **2013**, *6*, 2839.

[123] J. Liang, Y. Jiao, M. Jaroniec, S. Z. Qiao, *Angew. Chem. Int. Ed.* **2012**, *51*, 11496 – 11500; *Angew. Chem.* **2012**, *124*, 11664 – 11668.

[124] L. Zhang, Z. Xia, *J. Phys. Chem. C* **2011**, *115*, 11170 – 11176.

[125] J. Y. Cheon, J. H. Kim, J. H. Kim, K. C. Goddeti, J. Y. Park, S. H. Joo, *J. Am. Chem. Soc.* **2014**, *136*, 8875 – 8878.

[126] S. Wang, D. Yu, L. Dai, D. W. Chang, J.-B. Baek, *ACS Nano* **2011**, *5*, 6202 – 6209.

[127] M. Chokai, M. Taniguchi, S. Moriya, K. Matsubayashi, T. Shinoda, Y. Nabae, S. Kuroki, T. Hayakawa, M.-a. Kakimoto, J.-i. Ozaki, S. Miyata, *J. Power Sources* **2010**, *195*, 5947 – 5951.

[128] D. Wei, Y. Liu, Y. Wang, H. Zhang, L. Huang, G. Yu, *Nano Lett.* **2009**, *9*, 1752 – 1758.

[129] S. Maldonado, K. J. Stevenson, *J. Phys. Chem. B* **2005**, *109*, 4707 – 4716.

[130] S. Maldonado, S. Morin, K. J. Stevenson, *Carbon* **2006**, *44*, 1429 – 1437.

[131] H.-W. Liang, X. Zhuang, S. Brüller, X. Feng, K. Müllen, *Nat. Commun.* **2014**, *5*, 4973.

[132] a) K. Elumeeva, N. Fechler, T.-P. Fellinger, M. Antonelli, *Mater. Horiz.* **2014**, *1*, 588 – 594; b) J. P. Paraknowitsch, J. Zhang, D. Su, A. Thomas, M. Antonietti, *Adv. Mater.* **2010**, *22*, 87 – 92; c) L. Zhao, N. Baccile, S. Gross, Y. Zhang, W. Wei, Y. Sun, M. Antonietti, M.-M. Titirici, *Carbon* **2010**, *48*, 3778 – 3787.

[133] W. Yang, T.-P. Fellinger, M. Antonietti, *J. Am. Chem. Soc.* **2011**, *133*, 206 – 209.

[134] T.-P. Fellinger, F. Hasché, P. Strasser, M. Antonietti, *J. Am. Chem. Soc.* **2012**, *134*, 4072 – 4075.

[135] a) M.-M. Titirici, M. Antonietti, *Chem. Soc. Rev.* **2010**, *39*, 103 – 116; b) J. Zhang, S. Wu, X. Chen, M. Pan, S. Mu, *J. Power Sources* **2014**, *271*, 522 – 529; c) F. Pan, Z. Cao, Q. Zhao, H. Liang, J. Zhang, *J. Power Sources* **2014**, *272*, 8 – 15; d) R. J. White, N. Yoshizawa, M. Antonietti, M.-M. Titirici, *Green Chem.* **2011**, *13*, 2428 – 2434; e) G. Xu, J. Han, B. Ding, P. Nie, J. Pan, H. Dou, H. Li, X. Zhang, *Green Chem.* **2014**, *0*, 00; f) F. Liu, H. Peng, C. You, Z. Fu, P. Huang, H. Song, S. Liao, *Electrochim. Acta* **2014**, *138*, 353 – 359.

[136] Z. Lin, G. Waller, Y. Liu, M. Liu, C.-p. Wong, *Adv. Energy Mater.* **2012**, *2*, 884 – 888.

[137] S. Yasuda, L. Yu, J. Kim, K. Murakoshi, *Catal. Commun.* **2013**, *49*, 9627 – 9629.

[138] G.-L. Chai, Z. Hou, D.-J. Shu, T. Ikeda, K. Terakura, *J. Am. Chem. Soc.* **2014**, *136*, 13629 – 13640.

[139] S. M. Lyth, Y. Nabae, S. Moriya, S. Kuroki, M.-a. Kakimoto, J.-i. Ozaki, S. Miyata, *J. Phys. Chem. C* **2009**, *113*, 20148 – 20151.

[140] B. Winther-Jensen, O. Winther-Jensen, M. Forsyth, D. R. MacFarlane, *Science* **2008**, *321*, 671 – 674.

[141] M. S. Thorum, J. M. Hankett, A. A. Gewirth, *J. Phys. Chem. Lett.* **2011**, *2*, 295 – 298.

[142] L. Birry, J. H. Zagal, J. P. Dodelet, *Electrochem. Commun.* **2010**, *12*, 628 – 631.
[143] I. T. Bae, D. A. Tryk, D. A. Scherson, *J. Phys. Chem. B* **1998**, *102*, 4114 – 4117.
[144] D. Yu, L. Wei, W. Jiang, H. Wang, B. Sun, Q. Zhang, K. Goh, R. Si, Y. Chen, *Nanoscale* **2013**, *5*, 3457 – 3464.
[145] Z. Lin, M.-k. Song, Y. Ding, Y. Liu, M. Liu, C.-p. Wong, *Phys. Chem. Chem. Phys.* **2012**, *14*, 3381 – 3387.
[146] C. Domínguez, F. J. Pérez-Alonso, J. L. Gómez de La Fuente, S. A. Al-Thabaiti, S. N. Basahel, A. O. Alyoubi, A. A. Alshehri, M. A. Peña, S. Rojas, *J. Power Sources* **2014**, *271*, 87 – 96.
[147] K. Parvez, S. Yang, Y. Hernandez, A. Winter, A. Turchanin, X. Feng, K. Müllen, *ACS Nano* **2012**, *6*, 9541 – 9550.
[148] K. H. Lim, H. Kim, *Appl. Catal. B* **2014**, *158 – 159*, 355 – 360.
[149] H. Hu, B. Zhao, M. E. Itkis, R. C. Haddon, *J. Phys. Chem. B* **2003**, *107*, 13838 – 13842.
[150] I. W. Chiang, B. E. Brinson, R. E. Smalley, J. L. Margrave, R. H. Hauge, *J. Phys. Chem. B* **2001**, *105*, 1157 – 1161.
[151] A. R. Harutyunyan, B. K. Pradhan, J. Chang, G. Chen, P. C. Eklund, *J. Phys. Chem. B* **2002**, *106*, 8671 – 8675.
[152] C. Ge, F. Lao, W. Li, Y. Li, C. Chen, Y. Qiu, X. Mao, B. Li, Z. Chai, Y. Zhao, *Anal. Chem.* **2008**, *80*, 9426 – 9434.
[153] a) K.-D. Kreuer, S. J. Paddison, E. Spohr, M. Schuster, *Chem. Rev.* **2004**, *104*, 4637 – 4678; b) B. Smitha, S. Sridhar, A. A. Khan, *J. Membr. Sci.* **2005**, *259*, 10 – 26; c) B. C. Steele, A. Heinzel, *Nature* **2001**, *414*, 345 – 352.
[154] J. S. Spendelow, A. Wieckowski, *Phys. Chem. Chem. Phys.* **2007**, *9*, 2654 – 2675.
[155] a) S. Lu, J. Pan, A. Huang, L. Zhuang, J. Lu, *Proc. Natl. Acad. Sci. USA* **2008**, *105*, 20611 – 20614; b) J. R. Varcoe, R. C. T. Slade, *Fuel Cells* **2005**, *5*, 187 – 200; c) J. Pan, S. Lu, Y. Li, A. Huang, L. Zhuang, J. Lu, *Adv. Funct. Mater.* **2010**, *20*, 312 – 319; d) N. J. Robertson, H. A. Kostalik, T. J. Clark, P. F. Mutolo, H. D. Abruna, G. W. Coates, *J. Am. Chem. Soc.* **2010**, *132*, 3400 – 3404; e) S. Gu, R. Cai, T. Luo, Z. Chen, M. Sun, Y. Liu, G. He, Y. Yan, *Angew. Chem. Int. Ed.* **2009**, *48*, 6499 – 6502; *Angew. Chem.* **2009**, *121*, 6621 – 6624; f) J. Wang, S. Li, S. Zhang, *Macromolecules* **2010**, *43*, 3890 – 3896; g) Y. Liu, J. Wang, Y. Yang, T. M. Brenner, S. Seifert, Y. Yan, M. W. Liberatore, A. M. Herring, *J. Phys. Chem. C* **2014**, *118*, 15136 – 15145; h) M. A. Hickner, A. M. Herring, E. B. Coughlin, *J. Polym. Sci. Part B* **2013**, *51*, 1727 – 1735; i) J. R. Varcoe, R. C. T. Slade, E. Lam How Yee, *Chem. Commun.* **2006**, 1428 – 1429; j) J.-S. Park, S.-H. Park, S.-D. Yim, Y.-G. Yoon, W.-Y. Lee, C.-S. Kim, *J. Power Sources* **2008**, *178*, 620 – 626.
[156] G. Wu, C. M. Johnston, N. H. Mack, K. Artyushkova, M. Ferrandon, M. Nelson, J. S. Lezama-Pacheco, S. D. Conradson, K. L. More, D. J. Myers, P. Zelenay, *J. Mater. Chem.* **2011**, *21*, 11392 – 11405.
[157] F. H. B. Lima, J. Zhang, M. H. Shao, K. Sasaki, M. B. Vukmirovic, E. A. Ticianelli, R. R. Adzic, *J. Phys. Chem. C* **2007**, *111*, 404 – 410.
[158] a) J. Greeley, I. E. L. Stephens, A. S. Bondarenko, T. P. Johansson, H. A. Hansen, T. F. Jaramillo, J. Rossmeisl, I. Chorkendorff, J. K. Nørskov, *Nat. Chem.* **2009**, *1*, 552 – 556; b) G. Gupta, D. A. Slanac, P. Kumar, J. D. Wiggins-Camacho, X. Wang, S. Swinnea, K. L. More, S. Dai, K. J. Stevenson, K. P. Johnston, *Chem. Mater.* **2009**, *21*, 4515 – 4526; c) A. Sarkar, A. Manthiram, *J. Phys. Chem. C* **2010**, *114*, 4725 – 4732; d) C. Wang, M. Chi, D. Li, D. Strmcnik, D. van der Vliet, G. Wang, V. Komanicky, K.-C. Chang, A. P. Paulikas, D. Tripkovic, J. Pearson, K. L. More, N. M. Markovic, V. R. Stamenkovic, *J. Am. Chem. Soc.* **2011**, *133*, 14396 – 14403; e) I. Dutta, M. K. Carpenter, M. P. Balogh, J. M. Ziegelbauer, T. E. Moylan, M. H. Atwan, N. P. Irish, *J. Phys. Chem. C* **2010**, *114*, 16309 – 16320; f) R. Srivastava, P. Mani, N. Hahn, P. Strasser, *Angew. Chem. Int. Ed.* **2007**, *46*, 8988 – 8991; *Angew. Chem.* **2007**, *119*, 9146 – 9149; g) J. Zhang, F. H. Lima, M. H. Shao, K. Sasaki, J. X. Wang, J. Hanson, R. R. Adzic, *J. Phys. Chem. B* **2005**, *109*, 22701 – 22704; h) C. Koenigsmann, A. C. Santulli, K. Gong, M. B. Vukmirovic, W.-p. Zhou, E. Sutter, S. S. Wong, R. R. Adzic, *J. Am. Chem. Soc.* **2011**, *133*, 9783 – 9795.
[159] H.-S. Oh, H. Kim, *J. Power Sources* **2012**, *212*, 220 – 225.
[160] G. Nam, J. Park, S. T. Kim, D.-b. Shin, N. Park, Y. Kim, J.-S. Lee, J. Cho, *Nano Lett.* **2014**, *14*, 1870 – 1876.
[161] B. J. Kim, D. U. Lee, J. Wu, D. Higgins, A. Yu, Z. Chen, *J. Phys. Chem. C* **2013**, *117*, 26501 – 26508.
[162] H. Peng, F. Liu, X. Liu, S. Liao, C. You, X. Tian, H. Nan, F. Luo, H. Song, Z. Fu, P. Y. Huang, *ACS Catal.* **2014**, *4*, 3797 – 3805.
[163] B. Jeong, D. Shin, H. Jeon, J. D. Ocon, B. S. Mun, J. Baik, H.-J. Shin, J. Lee, *ChemSusChem* **2014**, *7*, 1289 – 1294.
[164] a) Y. Zhang, K. Fugane, T. Mori, L. Niu, J. Ye, *J. Mater. Chem.* **2012**, *22*, 6575 – 6580; b) T. C. Nagaiah, A. Bordoloi, M. D. Sánchez, M. Muhler, W. Schuhmann, *ChemSusChem* **2012**, *5*, 637 – 641.
[165] W. Xia, C. Jin, S. Kundu, M. Muhler, *Carbon,* DOI: 10.1016/j.carbon.2008.12.026.
[166] a) S. L. Gojković, S. Gupta, R. F. Savinell, *J. Electrochem. Soc.* **1998**, *145*, 3493 – 3499; b) A. Biloul, O. Contamin, G. Sacrbeck, M. Savy, D. Vandenham, J. Riga, J. J. Verbist, *J. Electroanal. Chem.* **1992**, *335*, 163 – 186.
[167] G. Faubert, R. Côté, J. P. Dodelet, M. Lefevre, P. Bertrand, *Electrochim. Acta* **1999**, *44*, 2589 – 2603.
[168] L. Trotochaud, S. L. Young, J. K. Ranney, S. W. Boettcher, *J. Am. Chem. Soc.* **2014**, *136*, 6744 – 6753.
[169] S. Gupta, C. Fierro, E. Yeager, *J. Electroanal. Chem.* **1991**, *306*, 239 – 250.
[170] Q. Wang, Z.-Y. Zhou, Y.-J. Lai, Y. You, J.-G. Liu, X.-L. Wu, E. Terefe, C. Chen, L. Song, M. Rauf, N. Tian, S.-G. Sun, *J. Am. Chem. Soc.* **2014**, *136*, 10882 – 10885.
[171] D. Singh, K. Mamtani, C. R. Bruening, J. T. Miller, U. S. Ozkan, *ACS Catal.* **2014**, *4*, 3454 – 3462.
[172] R. A. Rincón, J. Masa, S. Mehrpour, F. Tietz, W. Schuhmann, *Chem. Commun.* **2014**, *50*, 14760 – 14762.
[173] C. P. Jones, K. Jurkschat, A. Crossley, R. G. Compton, B. L. Riehl, C. E. Banks, *Langmuir* **2007**, *23*, 9501 – 9504.
[174] T. S. Olson, S. Pylypenko, J. E. Fulghum, P. Atanassov, *J. Electrochem. Soc.* **2010**, *157*, B54 – B63.
[175] P. H. Matter, E. Wang, J.-M. M. Millet, U. S. Ozkan, *J. Phys. Chem. C* **2007**, *111*, 1444 – 1450.
[176] R. Bashyam, P. Zelenay, *Nature* **2006**, *443*, 63 – 66.
[177] C. R. Venkateswara, Y. Ishikawa, *J. Phys. Chem. C* **2012**, *116*, 4340 – 4346.

Received: January 20, 2015
Published online: July 1, 2015